

A scanning electron micrograph (SEM) showing a dark, narrow, zig-zagging superconducting contact structure on a lighter, textured topological insulator substrate. The contact starts from the bottom left and extends towards the top right, with a slight bend in the middle. The background is a dark, grainy surface.

Superconducting Contacts to Topological Insulators

*David Goldhaber-Gordon
Stanford University
KITP, December 2011*

This talk is a snapshot of our understanding back in December

For this slide deck, I've only corrected minor typos and names in acknowledgments.

For a more recent and nuanced picture, with added data and analysis, please see:

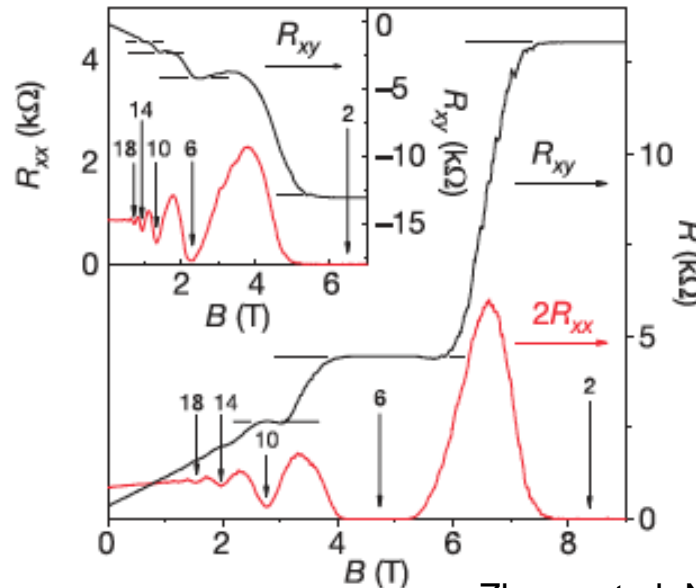
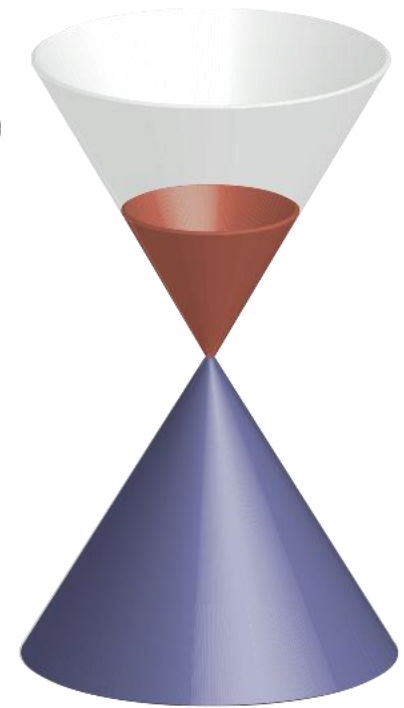
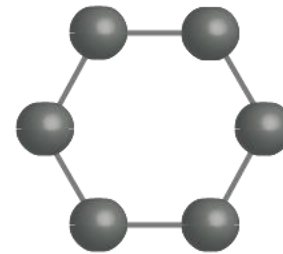
arXiv:1202.2323

Signatures of Majorana Fermions in Hybrid
Superconductor-Topological Insulator Devices

J. R. Williams, A. J. Bestwick, P. Gallagher, Seung Sae
Hong, Y. Cui, Andrew S. Bleich, J. G. Analytis, I. R. Fisher,
D. Goldhaber-Gordon

Novel 2DEGs: Dirac Particles

- New class of 2DEGs: Dirac Fermions. [cf. Klein Tunneling in Graphene, PRL **102** 026807 (2009)]
- In graphene, “Dirac” comes from symmetry of crystal structure
- Signatures of Dirac fermions can be seen in transport



$$E = \hbar ck$$

Novel 2DEGs: Dirac Particles and Spin-Orbit

- New class of Dirac systems:
Topological Insulators

Conduction Band

Valence Band

Novel 2DEGs: Dirac Particles and Spin-Orbit

- New class of Dirac systems:
Topological Insulators

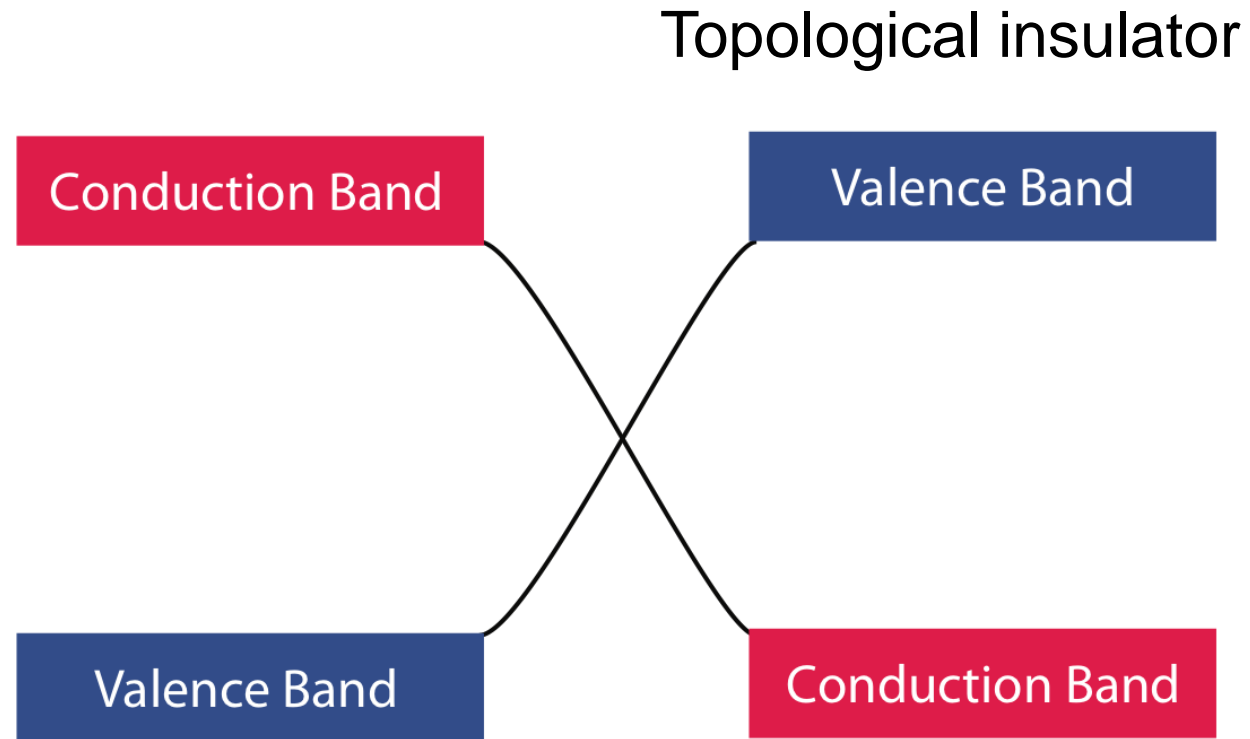
Topological insulator

Valence Band

Conduction Band

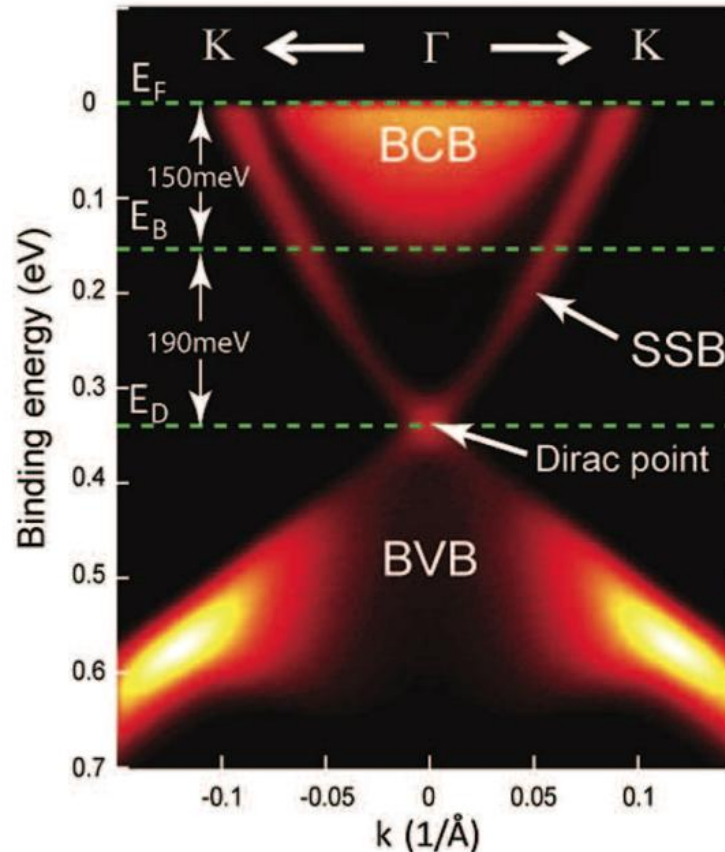
Novel 2DEGs: Dirac Particles and Spin-Orbit

- New class of Dirac systems: Topological Insulators
- Dirac arises from band inversion due to strong spin-orbit coupling
- More exotic particles possible: Majorana fermions, monopoles, etc.

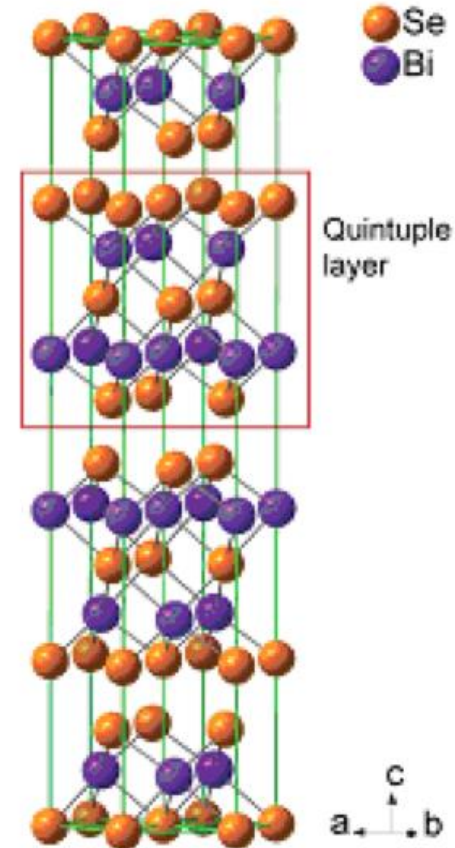


Novel 2DEG at the surface of a topological insulator: Bi_2Se_3

- Bi_2Se_3 can be grown as millimeter-scale crystals
- Surface states seen in surface-sensitive probes (ARPES, STM)
- Large gap ... but transport still includes bulk
- Layered structure, good for exfoliation



Y.L. Chen *et al.*, Science, 2010



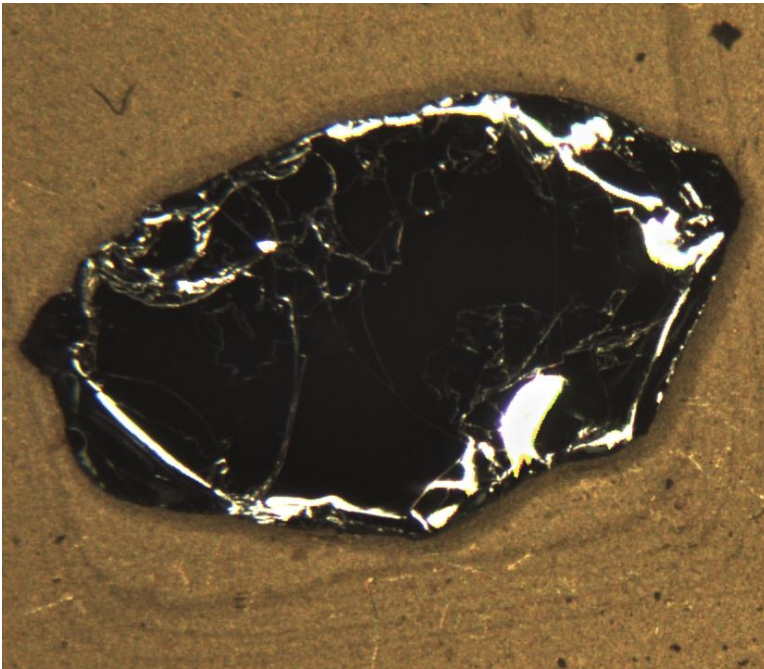
H. Peng *et al.*, Nano Lett., 2009

Outline

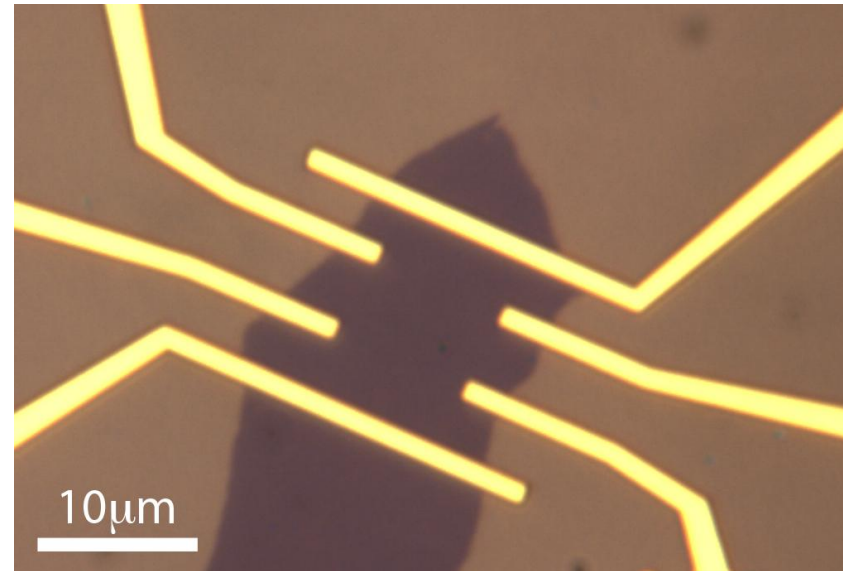
- Transport in ‘topologically-insulating’ materials
 - Materials growth and sample preparation
 - Gating: pushing around large charge densities
 - Methods to mitigate doping: materials and encapsulation
- Proximity-induced superconductivity in Bi_2Se_3
 - Sample Fabrication
 - S-TI-S junction dV/dI
 - Geometric dependence of critical current
 - Magnetic field dependence of critical current
 - What’s new and different?

Transport in Bi_2Se_3 and $\text{Bi}_2\text{Te}_2\text{Se}$

- Created nanometers-thin Bi_2Se_3 samples via mechanical exfoliation of thick Sn-doped Bi_2Se_3 crystals
- Pattern electrical leads with e-beam lithography

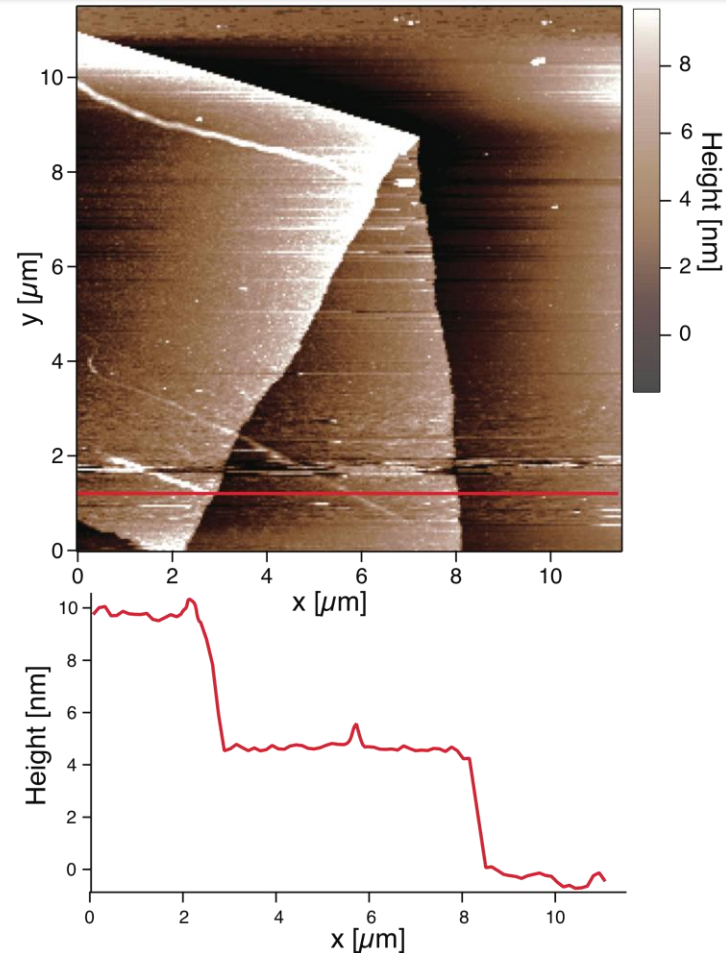


Exfoliation

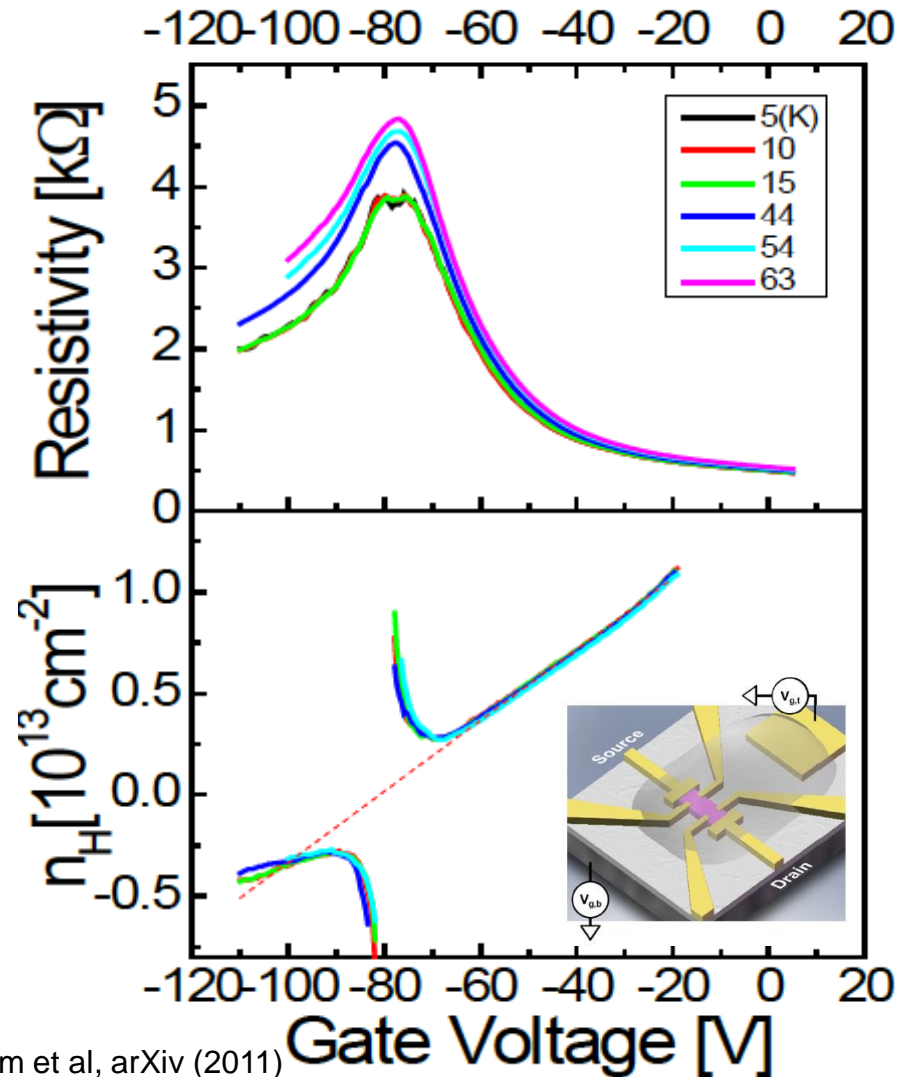
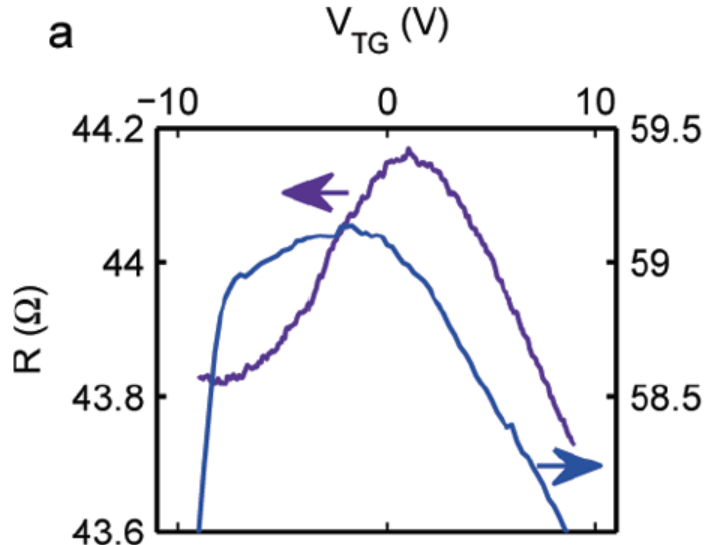
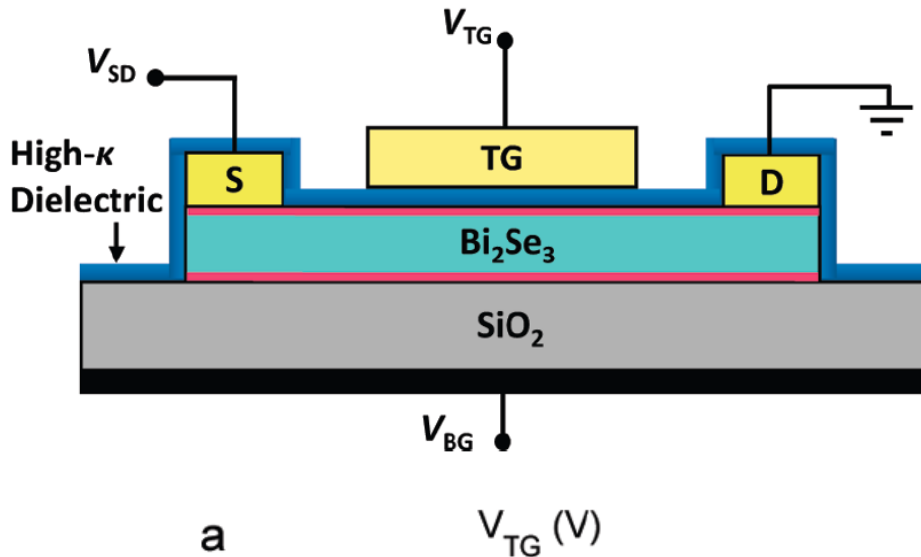


Atomically-flat exfoliated Bi_2Se_3

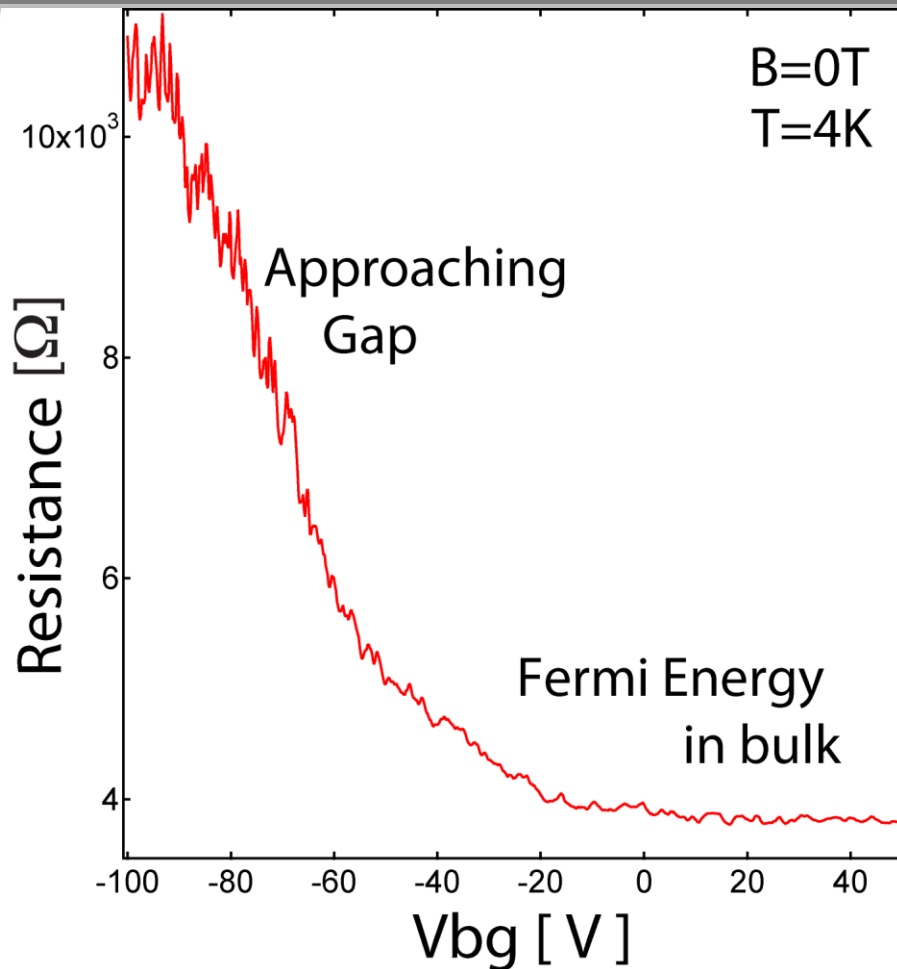
- AFM shows that flakes are often atomically flat and have lateral dimensions of many microns
- Thickness ranges from ~4nm to ~500nm



Getting to the Dirac Point

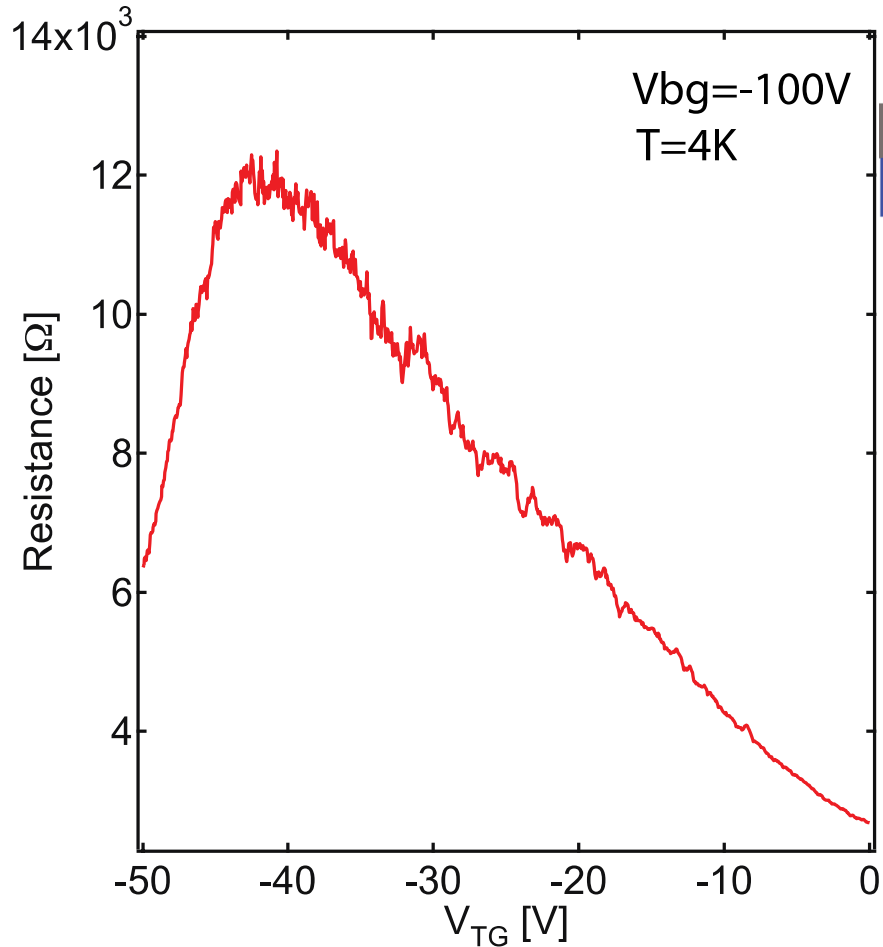


Our Work on Gating



- Thin samples (5-15 nm) highlight surface transport
- Chemical potential can be tuned via gate electrode
- But chemical potential not in bulk gap before gating

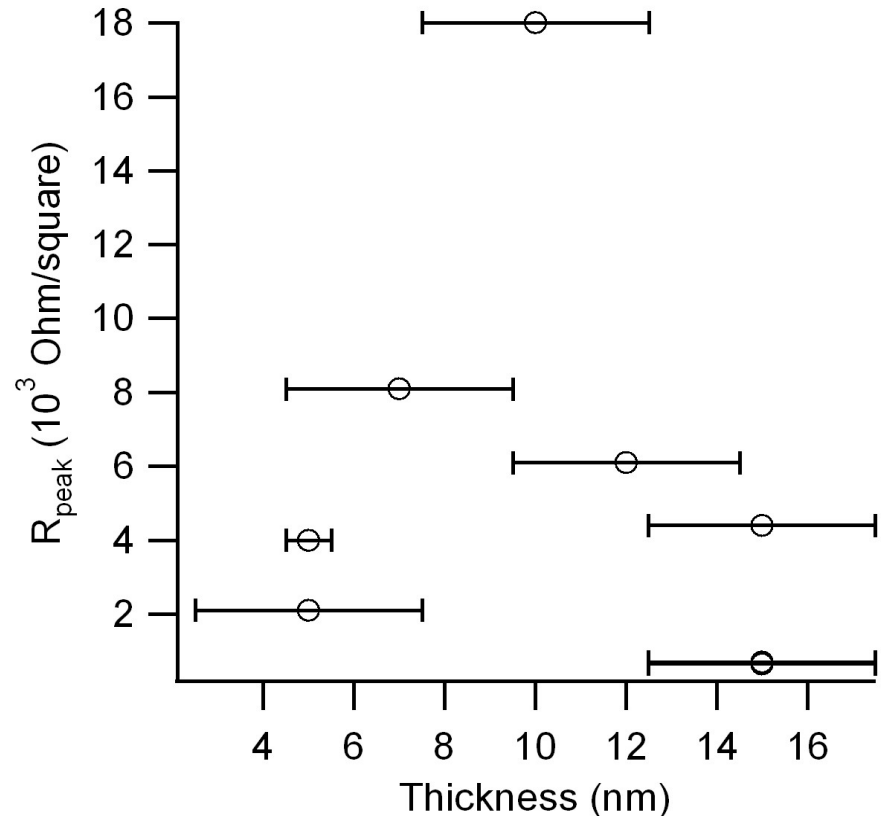
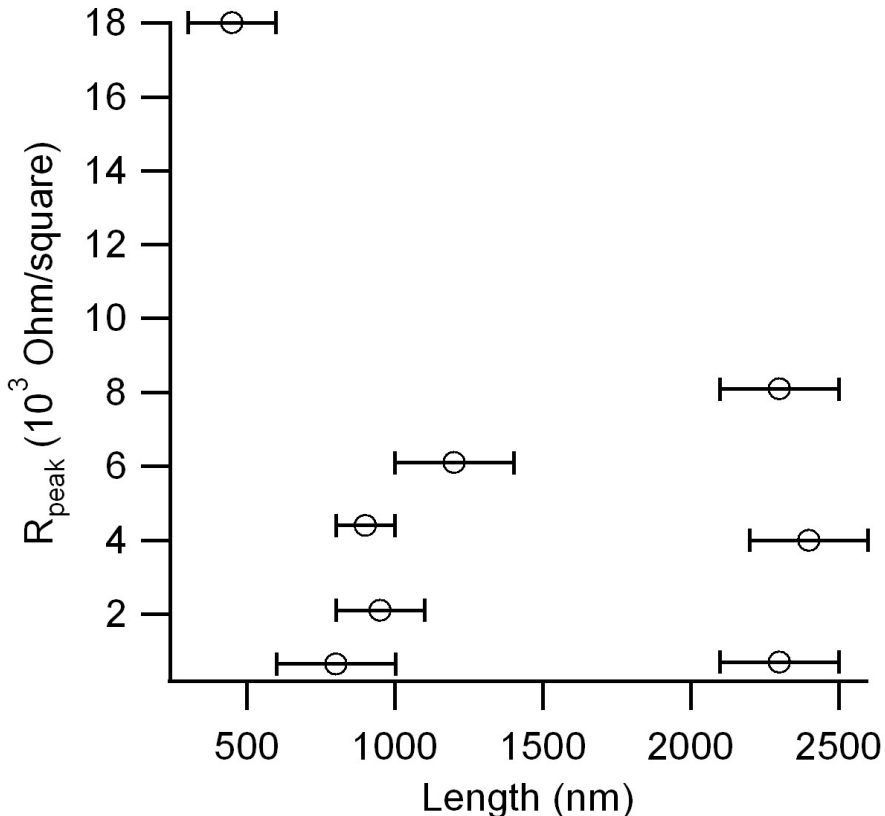
Double-Gated Devices



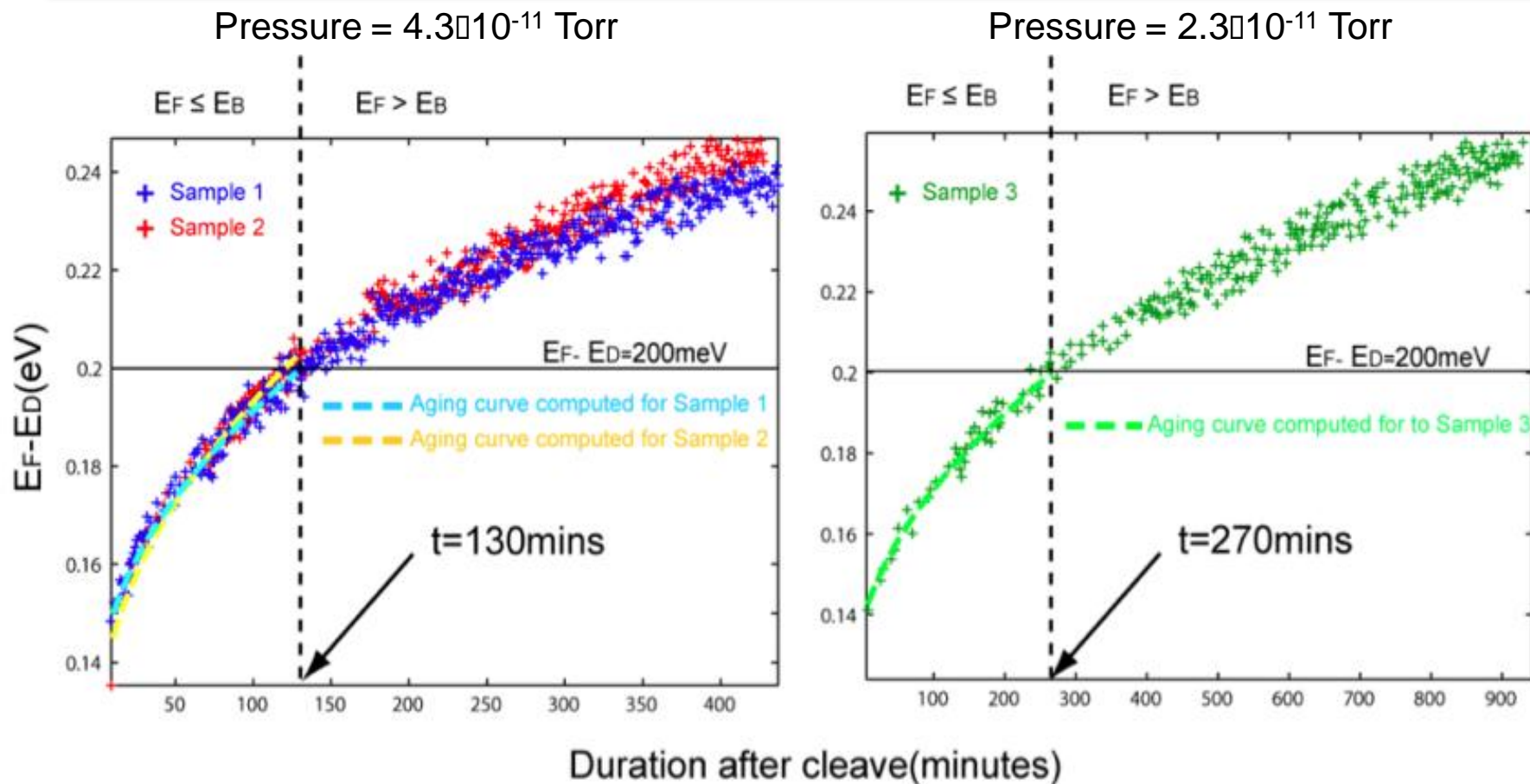
- Can achieve density swings of $\sim 10^{13} \text{ cm}^{-2}$.
- Observe peaks in resistance: presumably the peak occurs when the Fermi energy crosses the Dirac point.
- Magnetic field has little effect, likely due to the low mobility (high impurity doping).

Summary of Devices

- Resistance peak vs. gate voltage in 8 devices of various lateral geometries, aspect ratios and thickness
- Peak resistance independent of device geometry

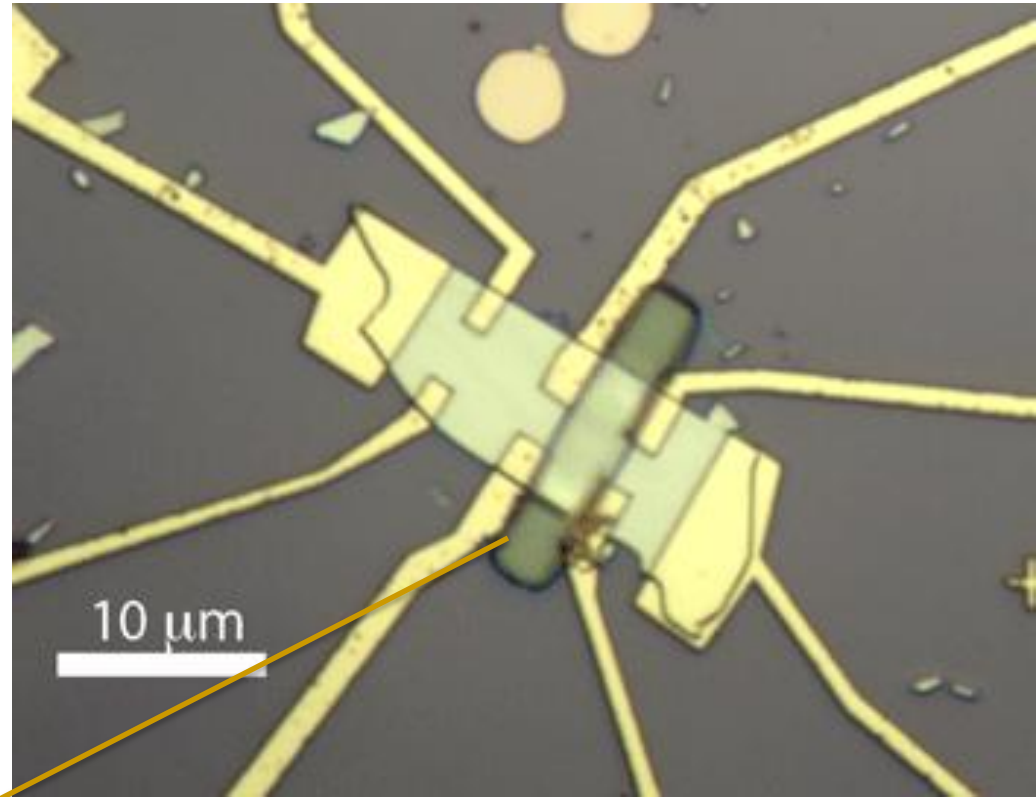


A Culprit: Exposure to Air



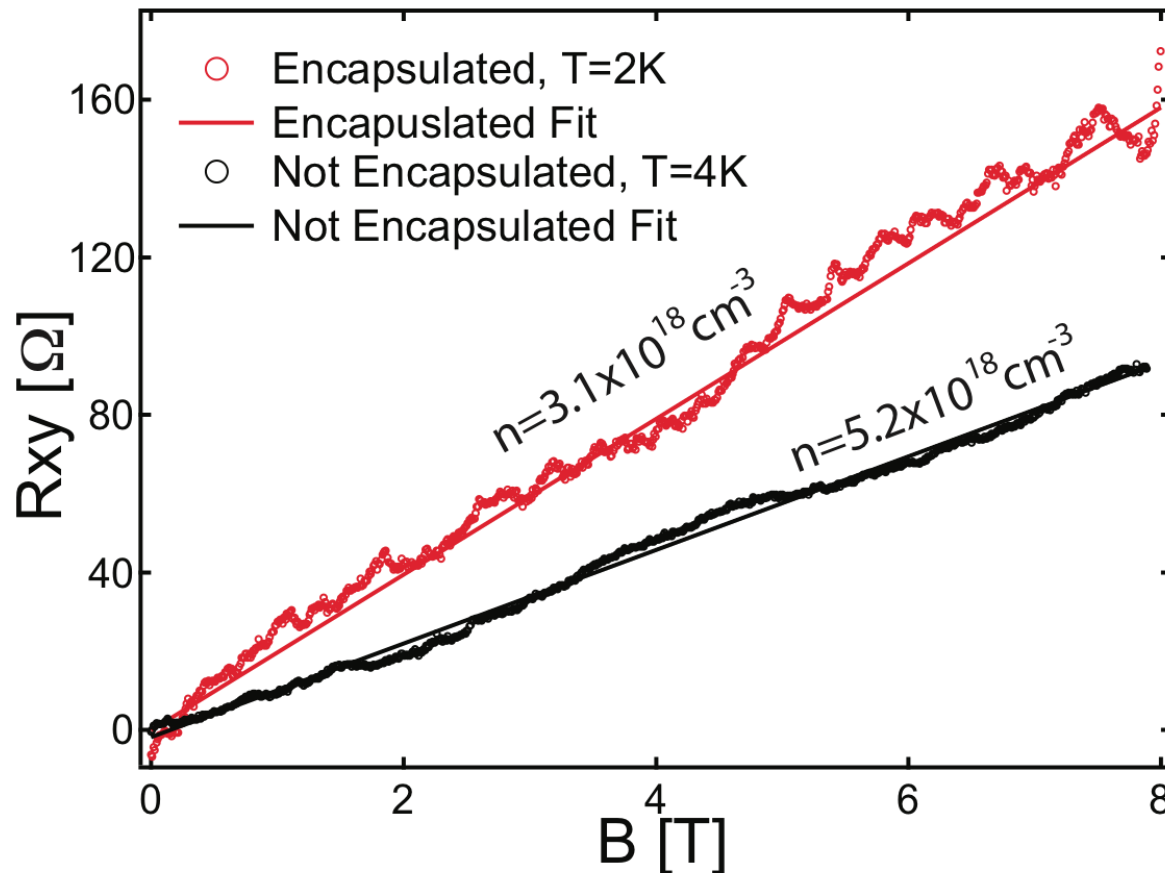
Device Encapsulation

- Cover device with a hydrophobic material to prevent water doping (surface, electron doping) of the device.
- Devices are exfoliated in a glove box and covered with PDMS.
- E-beam lithography allows for the definition of the covered area.
- Can measure transport in the covered and uncovered areas.



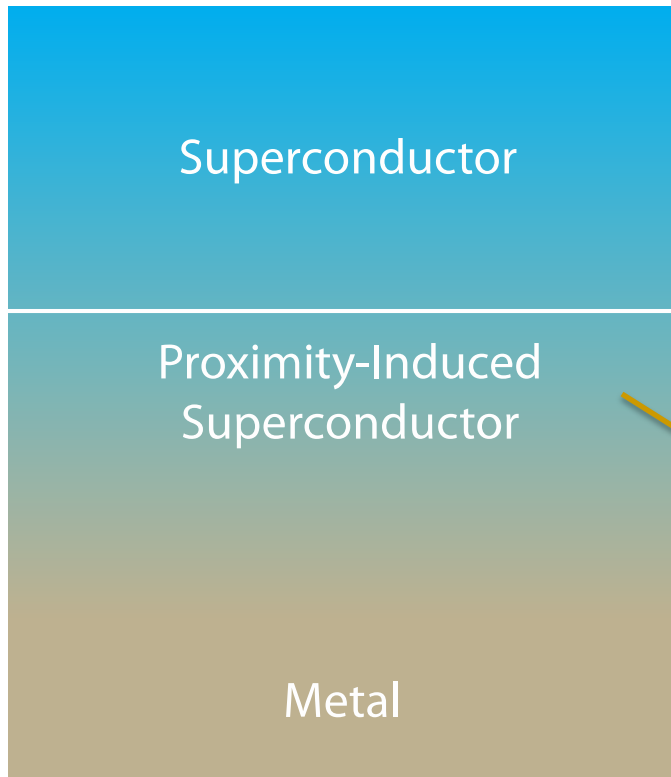
PDMS

Density modification by encapsulation



- Encapsulation lowers measured density (for a device thickness of 100nm).
- Assuming difference between two regions is entirely in the top ~ 10 nm, density near surface is reduced by a factor of 10

Adding interaction between carriers – the proximity effect

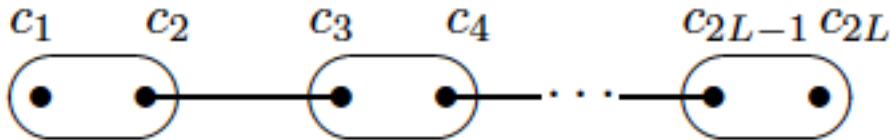
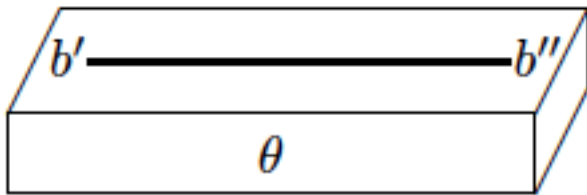


- Can induce extra correlations between electrons by placing a material in proximity to a superconductor
- Resulting system a “hybrid” of the two systems

$$H_{PROX} = K_{METAL} + \Delta_{SUPER} \psi^+ \psi$$

Zero Energy Modes in Superconductors

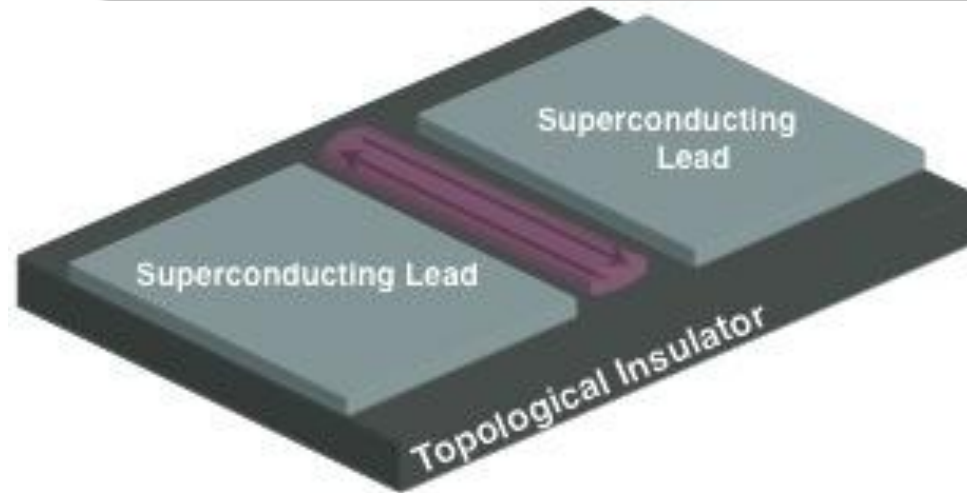
1D quantum wire on a 3D p+ip superconductor



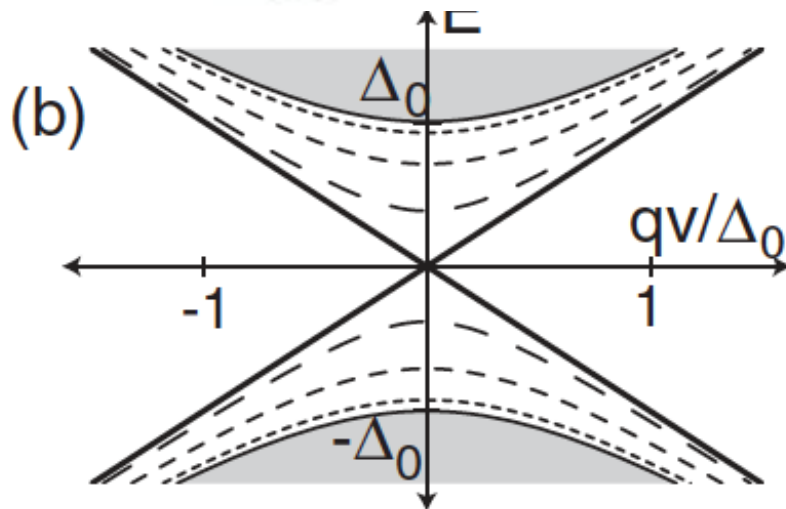
Kitaev, arXiv:condmat/0010440

- Can get situations in superconductors where particle excitations are the same as the antiparticle excitations. But you can't use just any superconductor
- Kitaev showed that under certain conditions for 1D p+ip superconductors you can have unpaired Majorana fermions at the end of the wire

Topological Insulators and the Proximity Effect



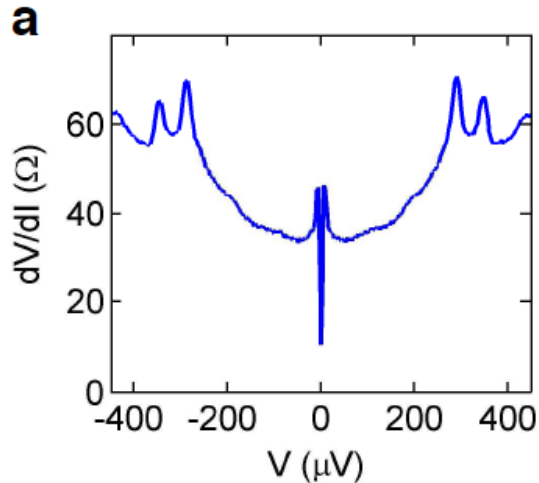
- Topological superconductors (or proximity-induced SC in TI) similar to p+ip superconductors
- 2D: localized Majoranas of the previous case become 1D wire
- 1D wire exists between the superconducting contacts (S)
- Gapless modes for phase difference of π between the leads



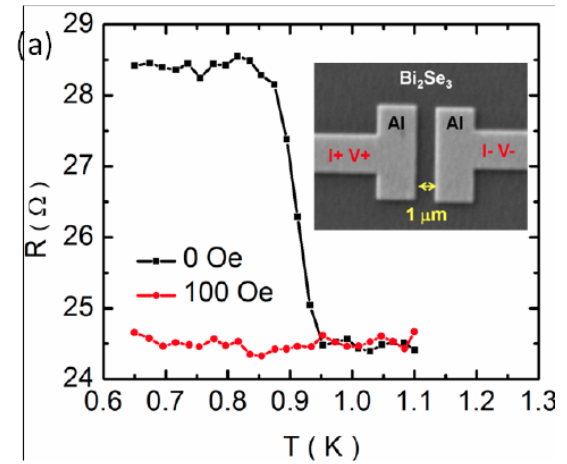
Fu and Kane, PRL, 2008

Titov, Ossipov & Beenakker PRB, 2007

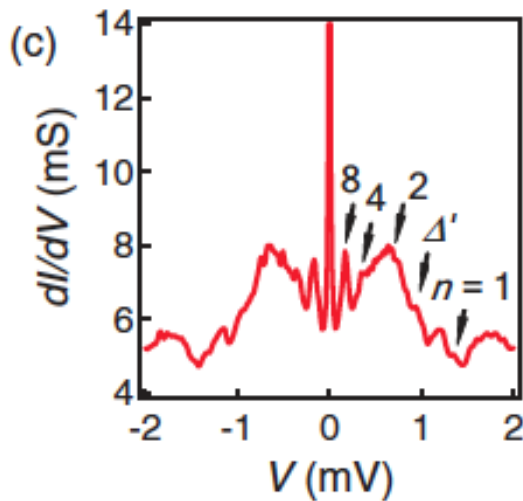
What's been measured



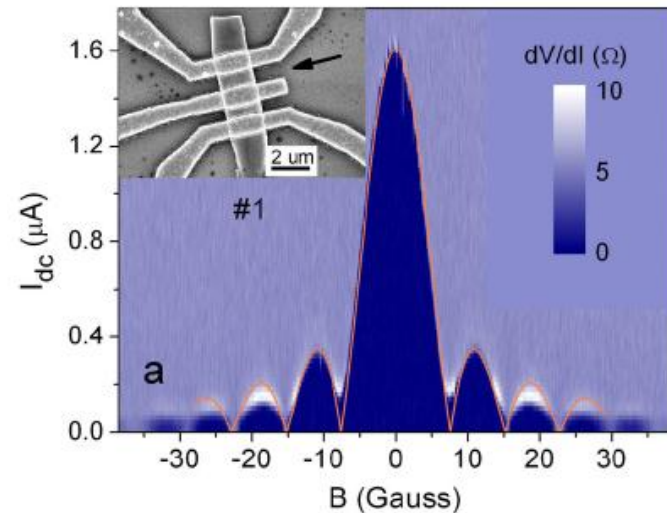
Sacepe et al., arXiv (2011)



Wang et al., arXiv (2011)

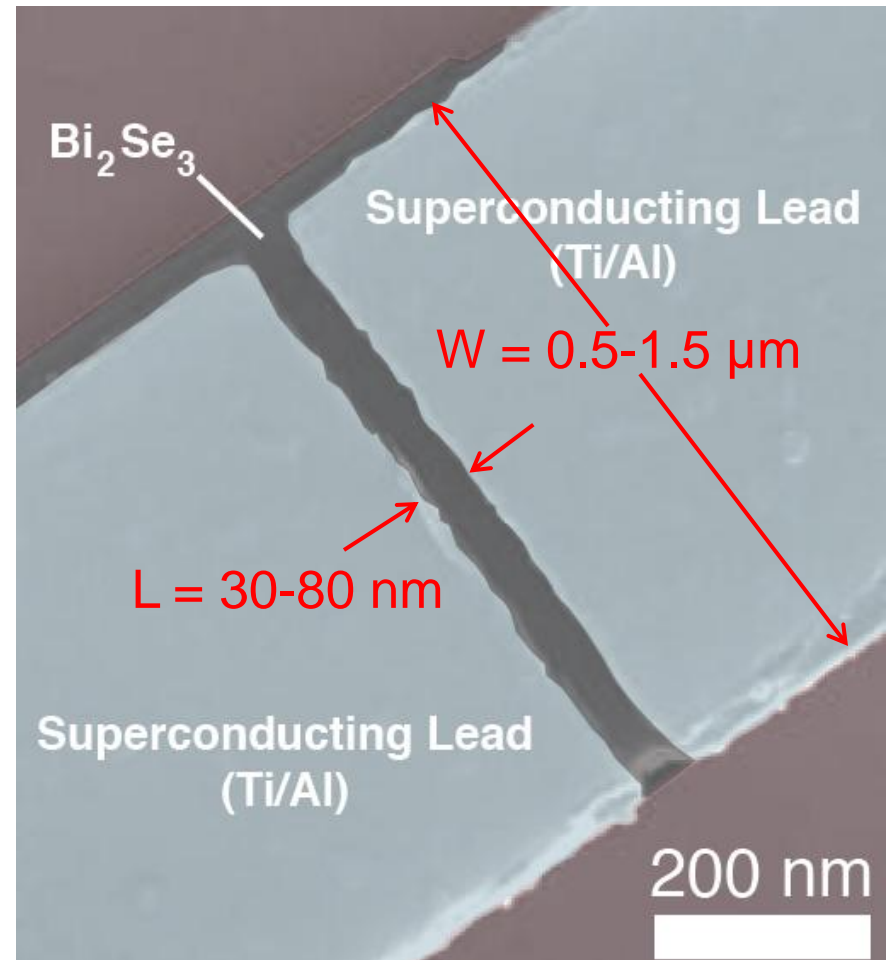
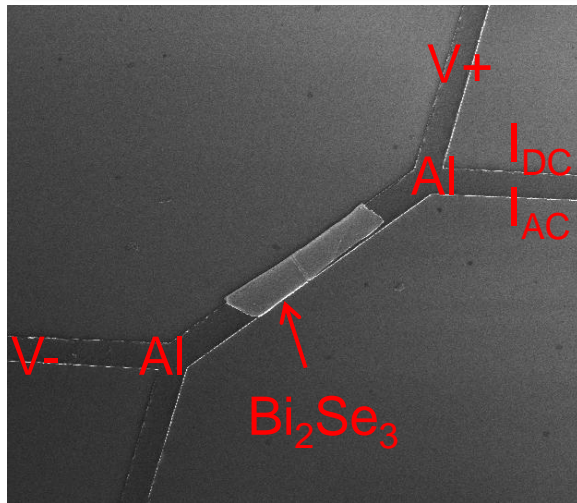


Zhang et al., PRB (2011)



Qu et al., arXiv (2011)

Superconducting Contacts on Bi₂Se₃

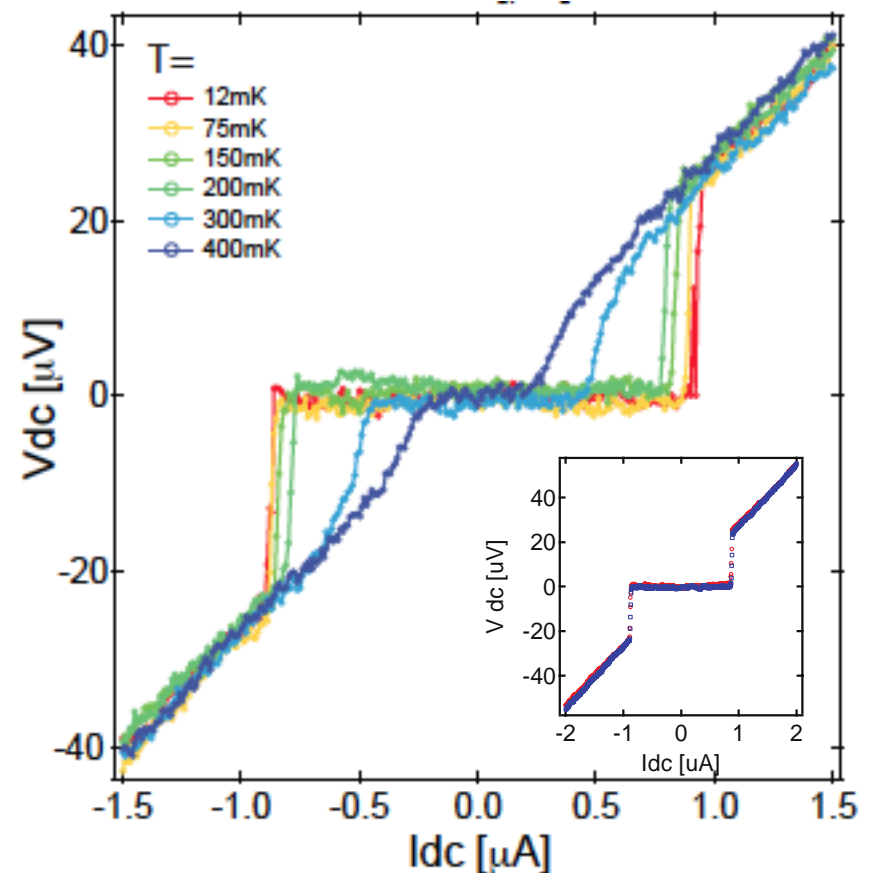
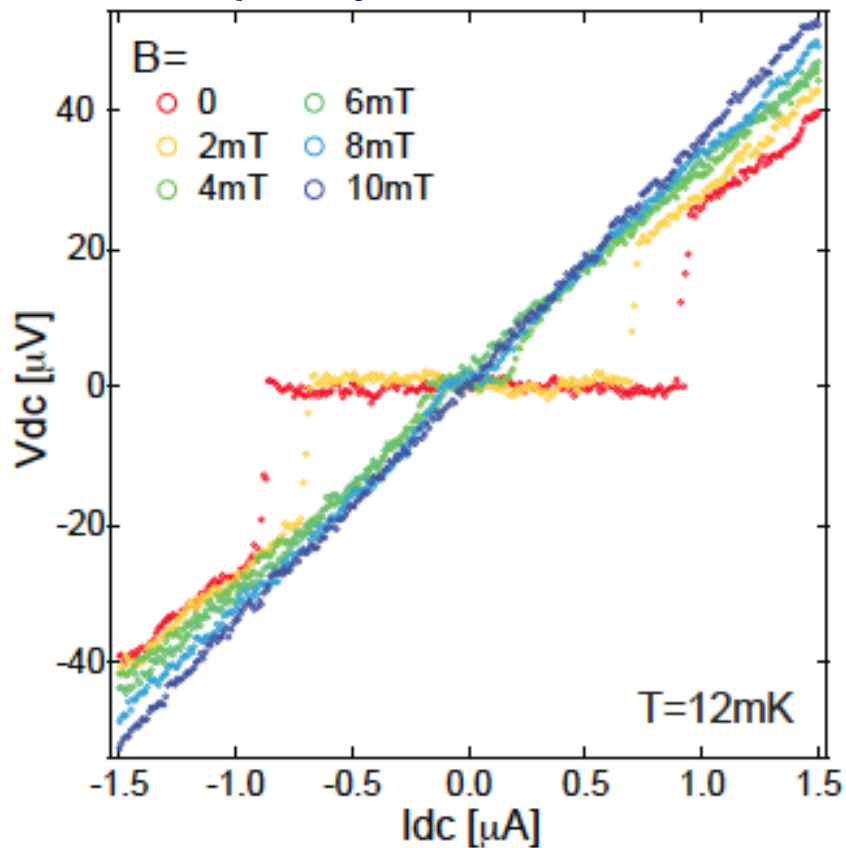


- Exfoliated flakes, thickness ~100nm
- Electrical contacts: Ti/Al 2nm/60nm
- Surface quantum scattering length ~ 200nm*

*Qu *et al.*, Science, 2010

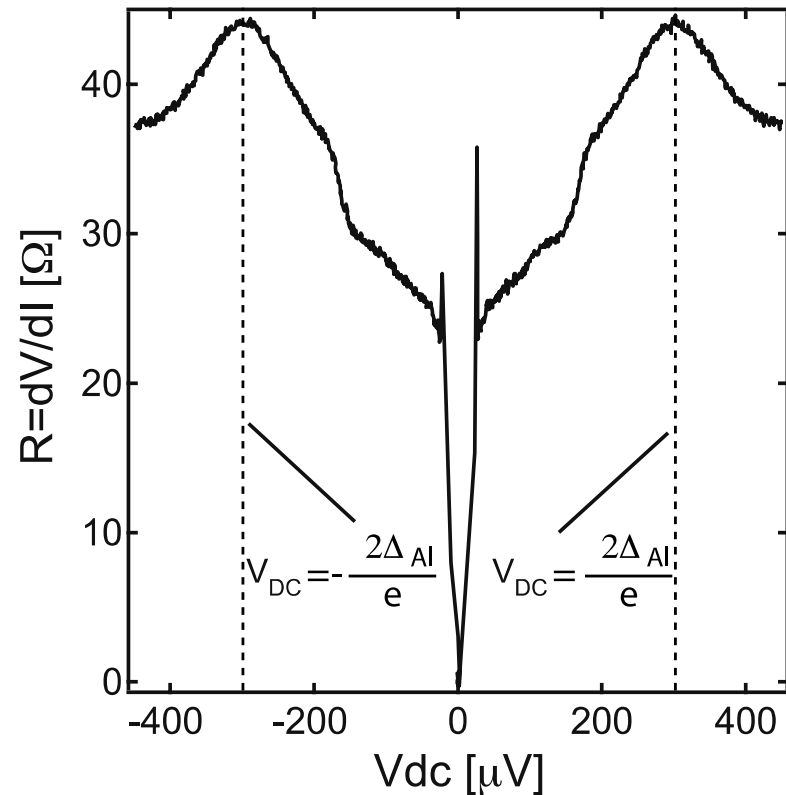
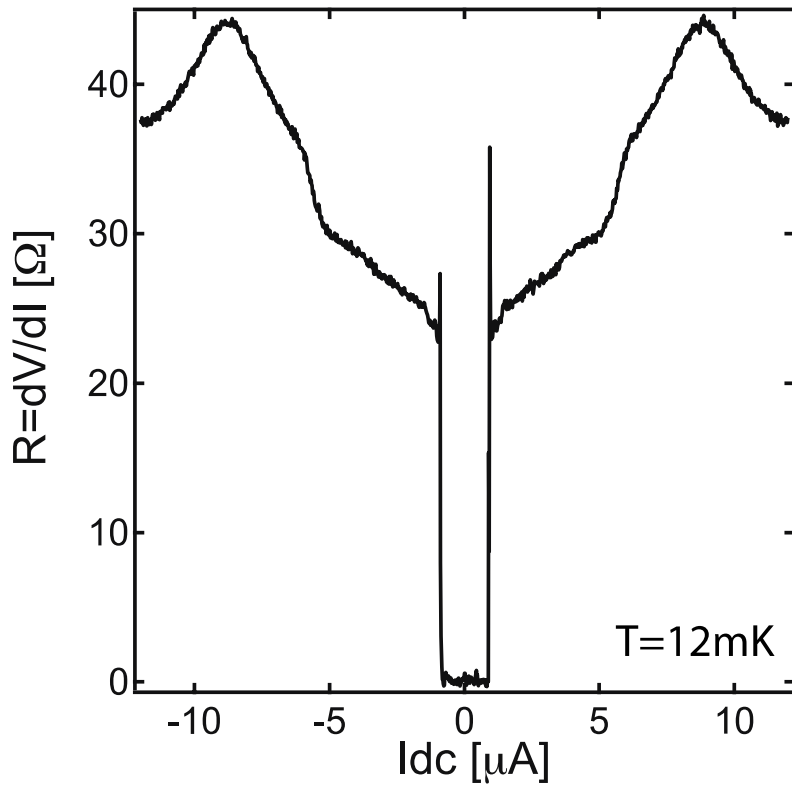
Supercurrent in Bi_2Se_3 Josephson Junction

- Temperature and magnetic field dependence of the DC response of the junction. Note no hysteresis \rightarrow overdamped junction



Supercurrent in Bi_2Se_3

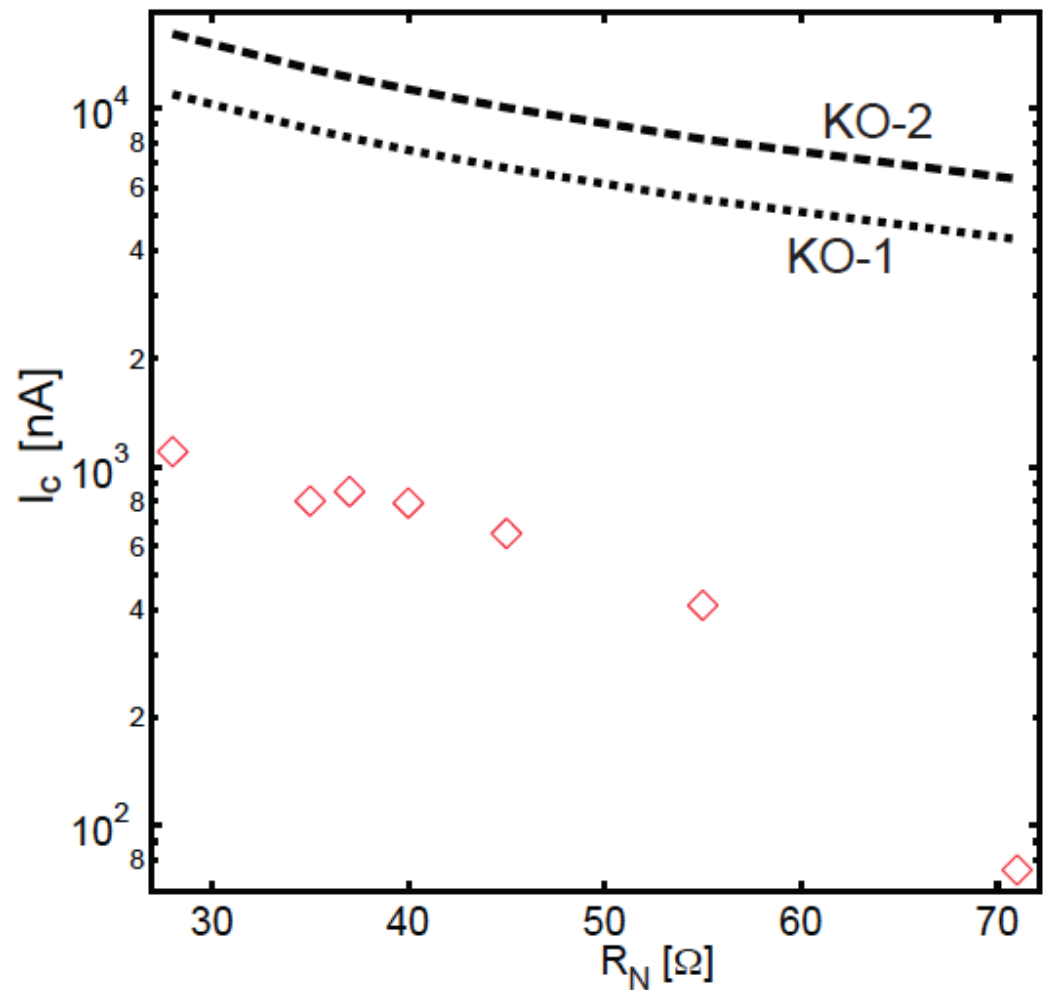
Josephson Junction: Differential



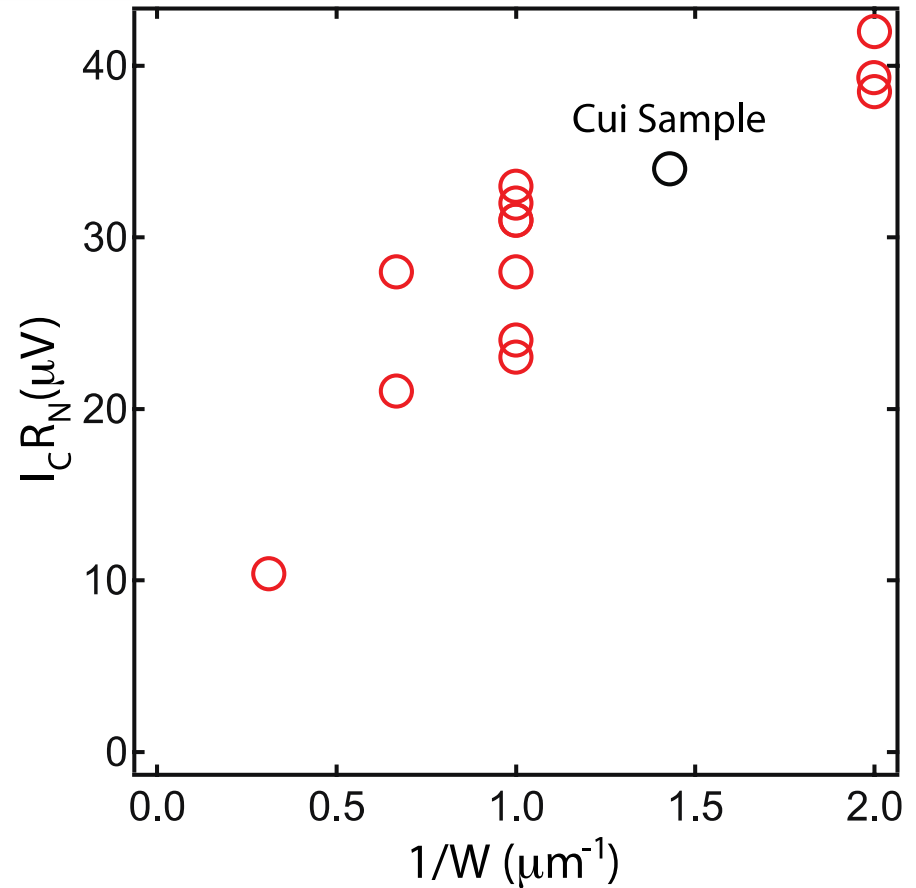
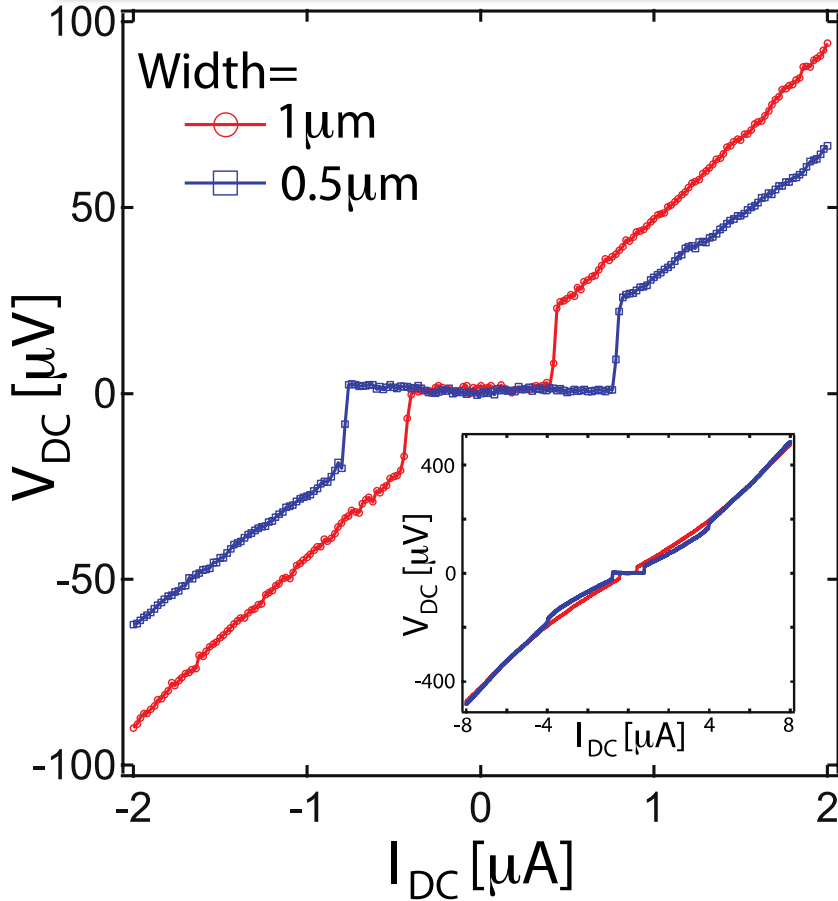
- Left: Current-bias, right: voltage across junction. Features in dV/dI at 2Δ and others below 2Δ .

Critical Currents too low

- Critical currents a factor of ten lower than what is expected from KO theory
- Sources of low critical current (neither apply)
 - Thermal effects – bad filter
 - Junction much longer than the coherence length



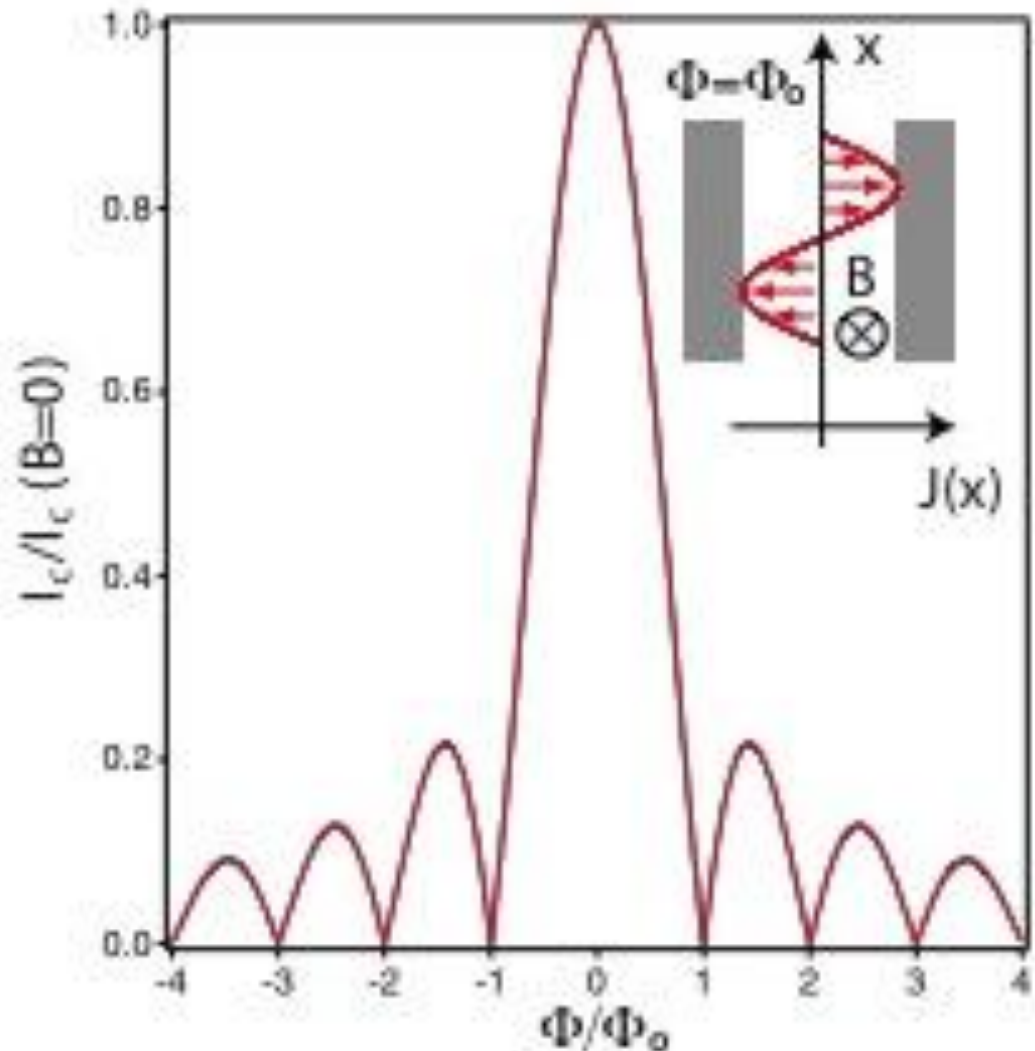
1/W dependence of $I_C R_N$



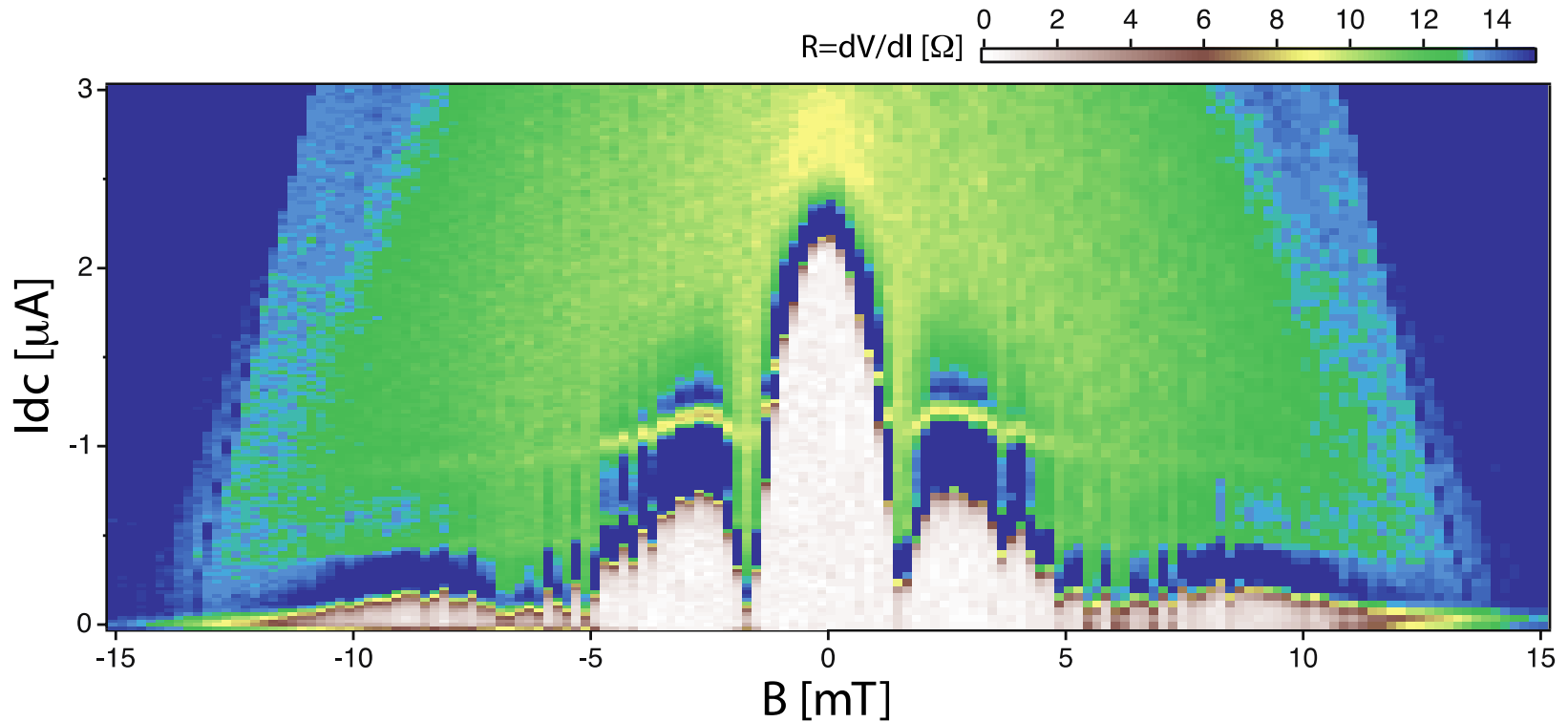
- Left: I-V curves for two devices with similar R_N
- Scaling of $I_C R_N$ for all 14 devices we've measured so far.

Magnetic-field dependence of I_c for standard JJ

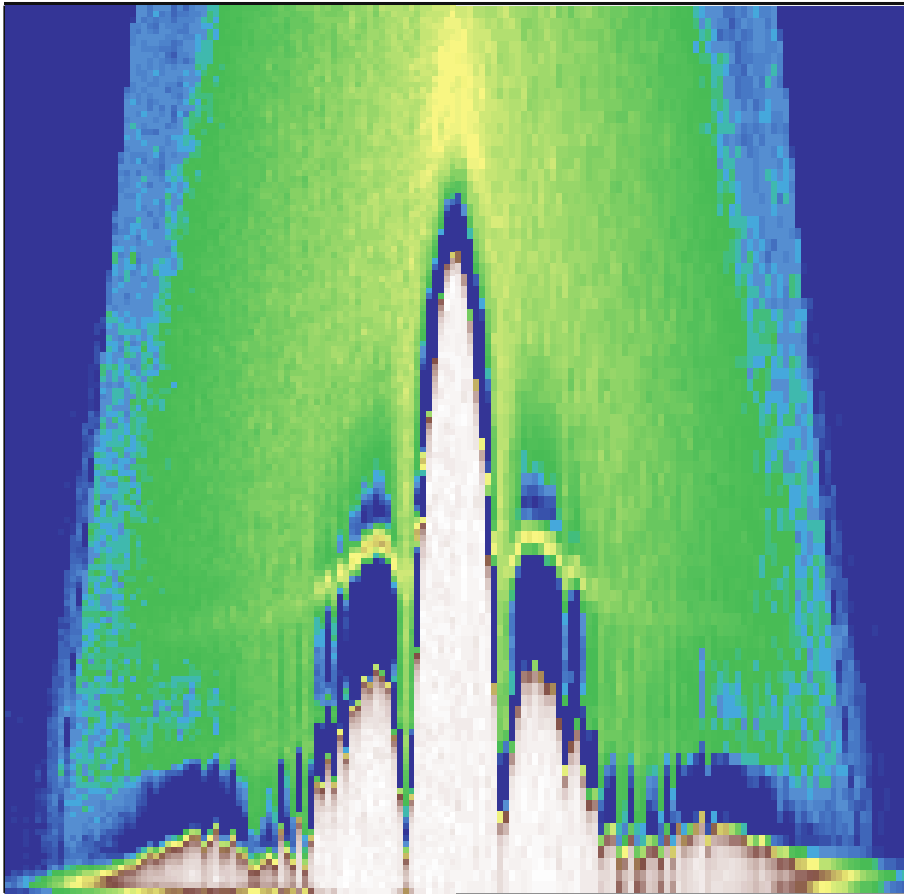
- Fraunhofer pattern expected for measurement of critical current vs. magnetic field
- Magnetic field scale set by device area



Magnetic-field dependence for Bi_2Se_3 junctions

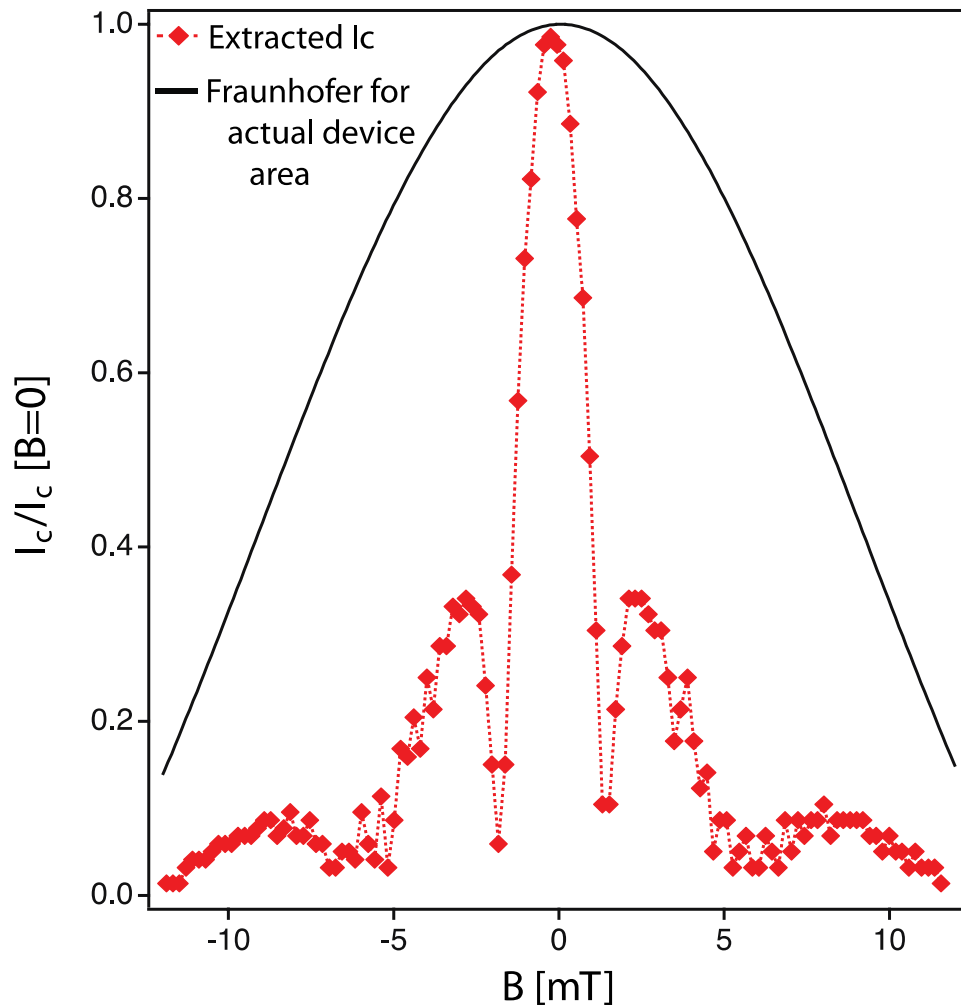


Magnetic-field dependence for Bi_2Se_3 junctions



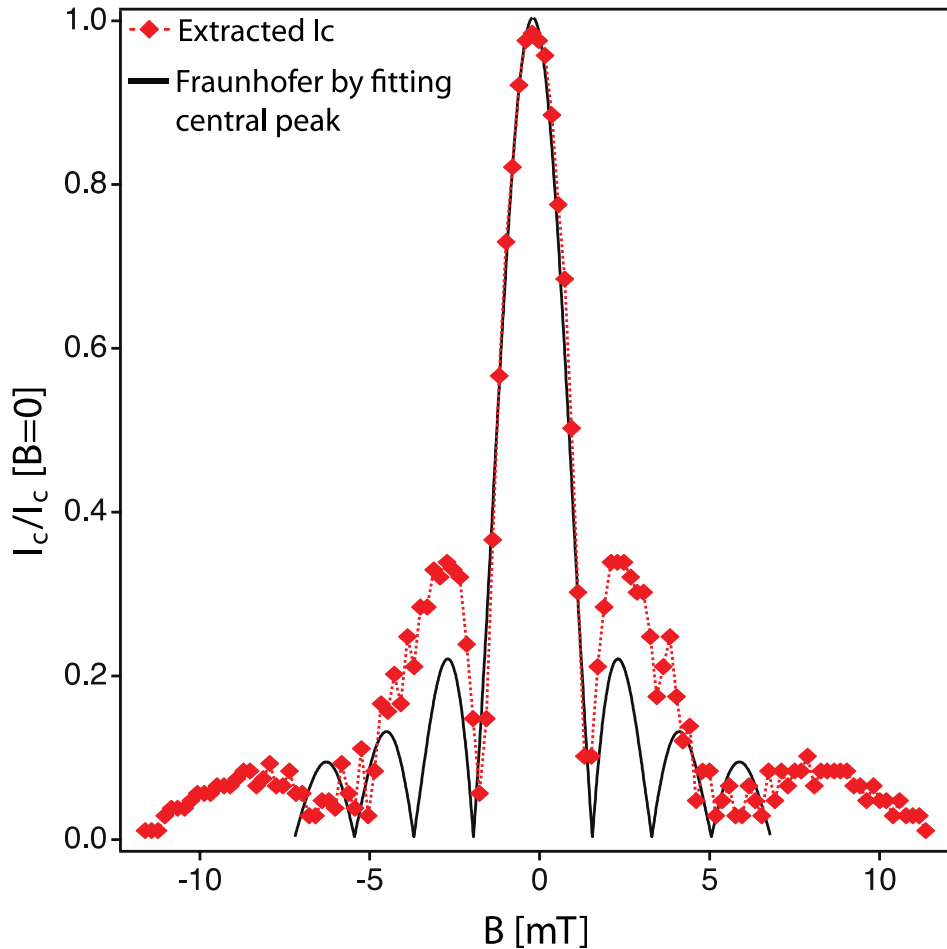
- Three distinct features in this plot
 - Field scale is wrong for the device size
 - Not Fraunhofer
 - Additional features observed that aren't expected

Magnetic-field dependence: Field scale



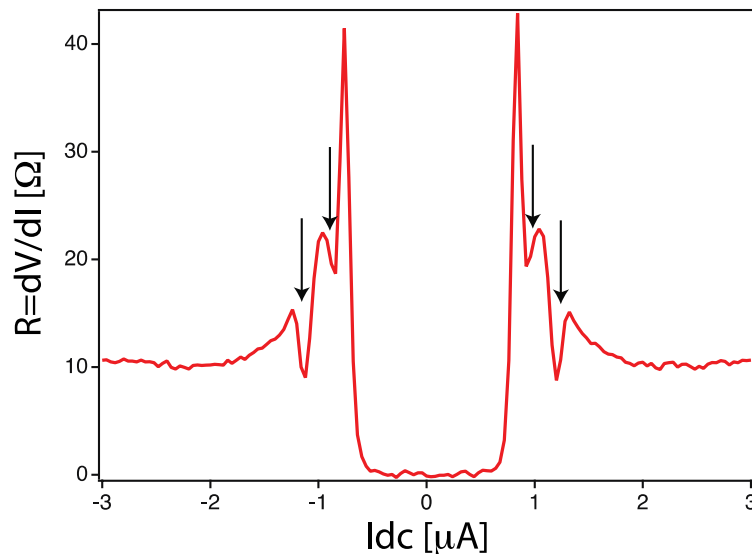
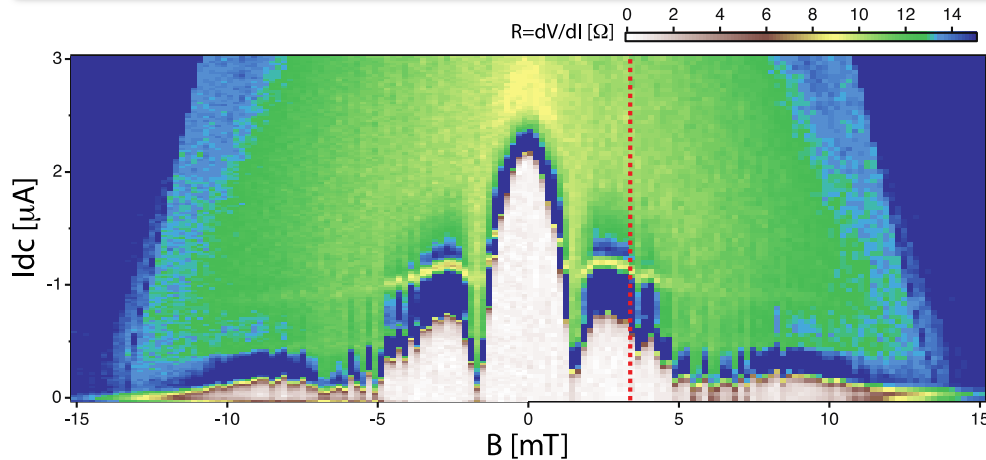
- Black line: Calculated Fraunhofer pattern for device geometry (including penetration depth)
- Scale off for all devices by a factor of ~ 5 .

Magnetic-field dependence: Field scale



- Black line: Calculated Fraunhofer pattern obtained by fitting the central peak
- The spacing of the lobes is 2 times larger than it should be, given the width of the central peak

Magnetic-field dependence: Additional Features

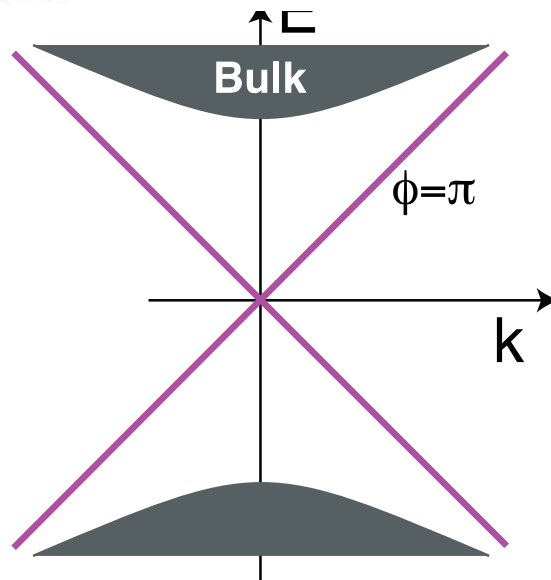
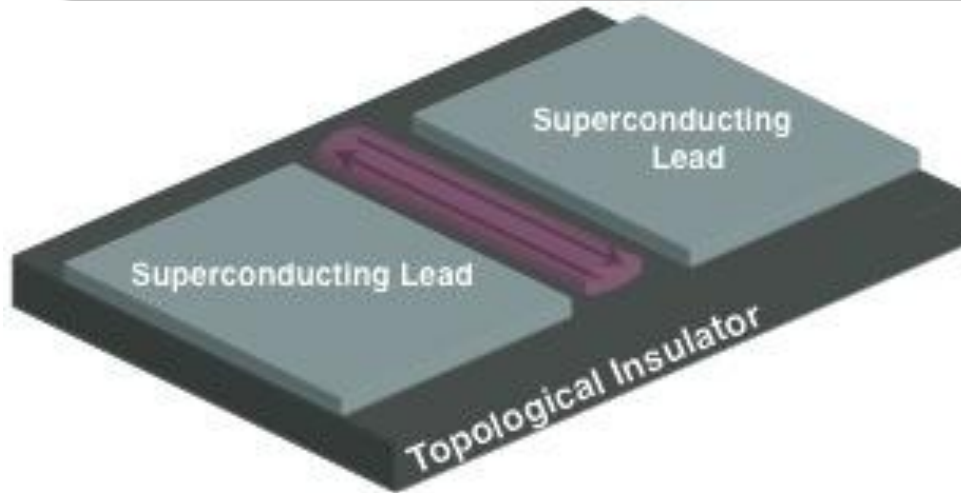


- Above I_C , for magnetic fields outside the first lobe, there are two symmetric “shadow” dips that follow the I_C curve
- Shadow effect symmetry about zero DC current

Key features that we need to understand

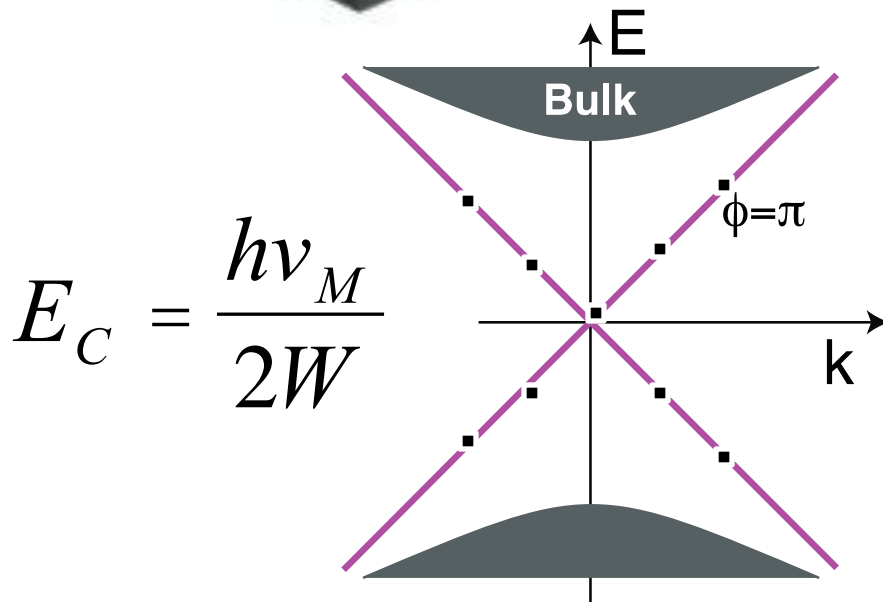
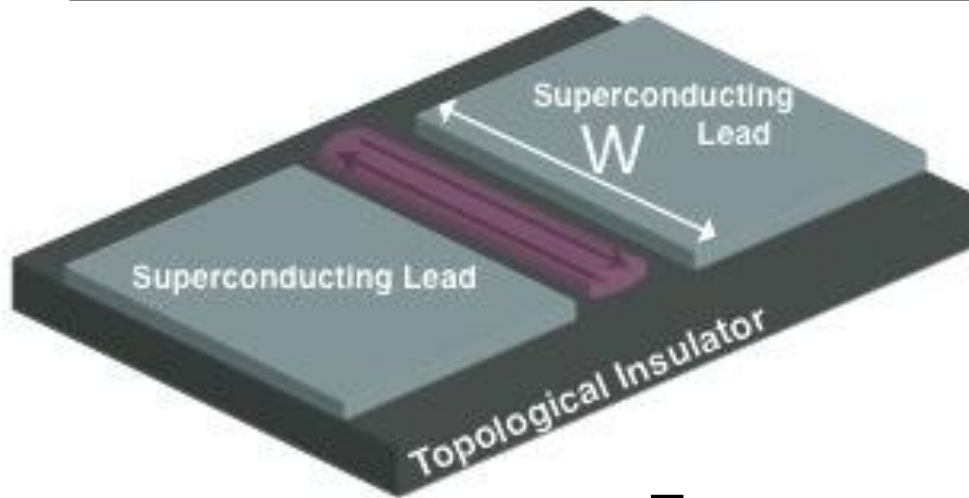
- The product $I_C R_N$ is too small, by a factor of about 10
- There is a trend in the product $I_C R_N$; scales as $1/W$
- The magnetic field scale and period is inconsistent with typical Josephson Junction behavior

Returning to Fu/Kane



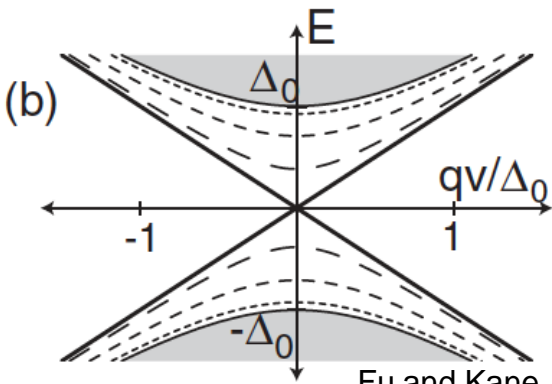
- For a phase difference of π , there is a gapless Majorana mode with zero energy
- This mode is the lowest lying energy state in the junction
- How does it interact with supercurrent?

Potential Explanation: 1D wire of Majorana fermions

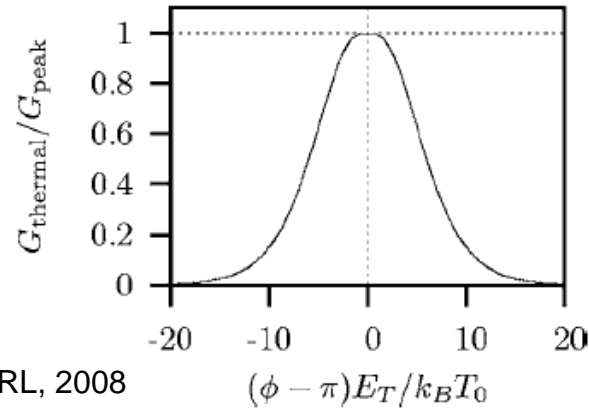


- For micron sized wire, confinement will occur along the wire
- The confinement will be set by the width of the Josephson Junction
- If the Majorana is dissipative, at energies of $E_C = eV_C$, the device will cease to superconduct
- Explains $1/W$ dependence
- A fit $V_C = I_C R_N$ to gives a velocity of 10^4m/s . This is close to the estimate for some but not all predictions for the Majorana velocity

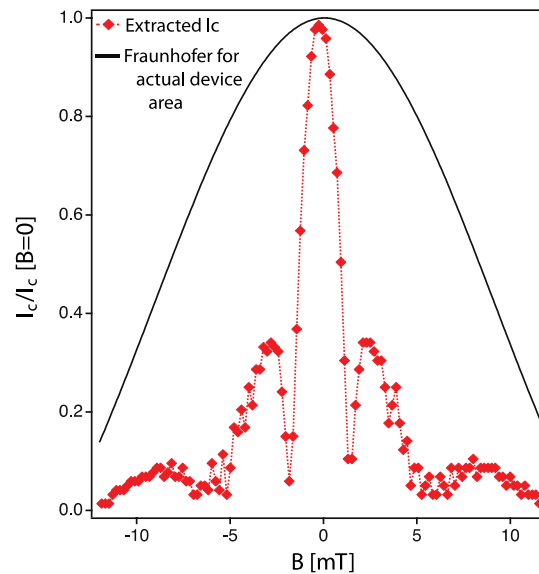
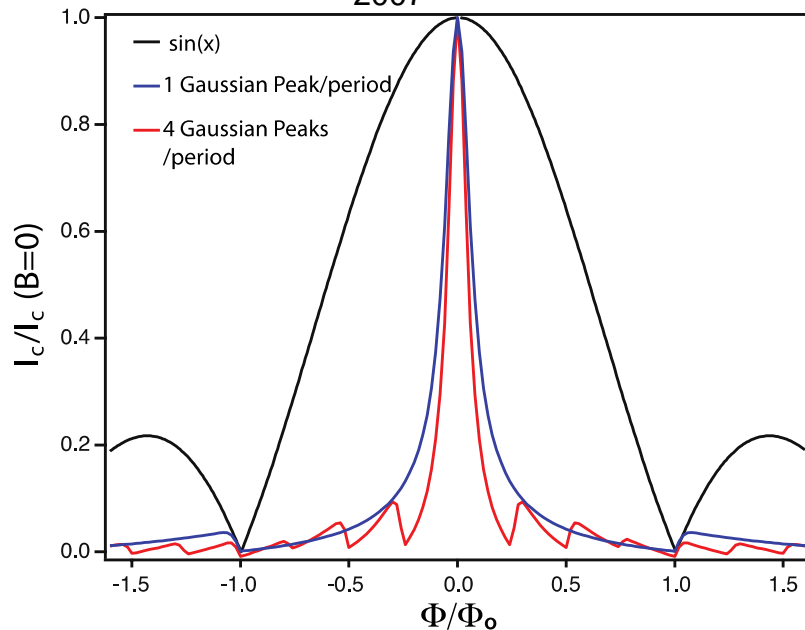
Narrowing of the field dependence



Fu and Kane, PRL, 2008
Titov, Ossipov & Beenakker PRB, 2007



- A peaked current vs. ϕ can give a narrowing of the magnetic field dependence



Conclusions

- Have shown gateability of topological insulator materials
- From these measurements, we've seen that the surface can contribute significantly to transport
- We have made measurements on superconducting devices in the quasiballistic regime
- Junctions of Bi_2Se_3 show many departures from conventional junction
- These departures were explain in terms of gapped 1D Majorana wire in the junction

Acknowledgments

Measurements

- James Williams
- Andrew Bestwick
- Patrick Gallagher

Growth

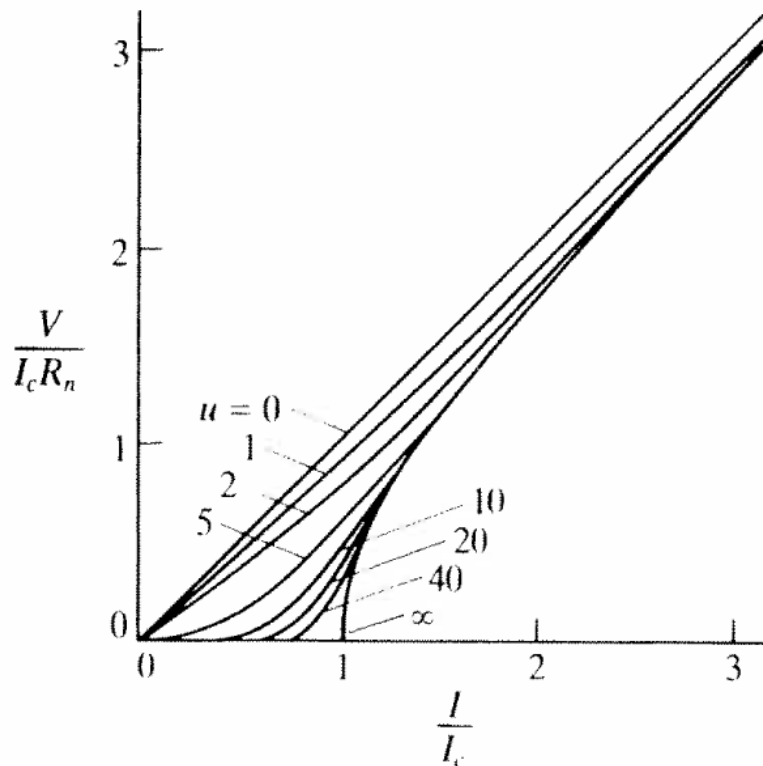
- James Analytis
- Andrew Bleich
- Ian Fisher
- Seung Sae Hong
- Yi Cui

Useful Conversations

- Jed Johnson
- John Clarke
- Mac Beasley
- Xiaoliang Qi

Thermal Noise Effects

Over-Damped Junctions: Ambegaokar-Halperin



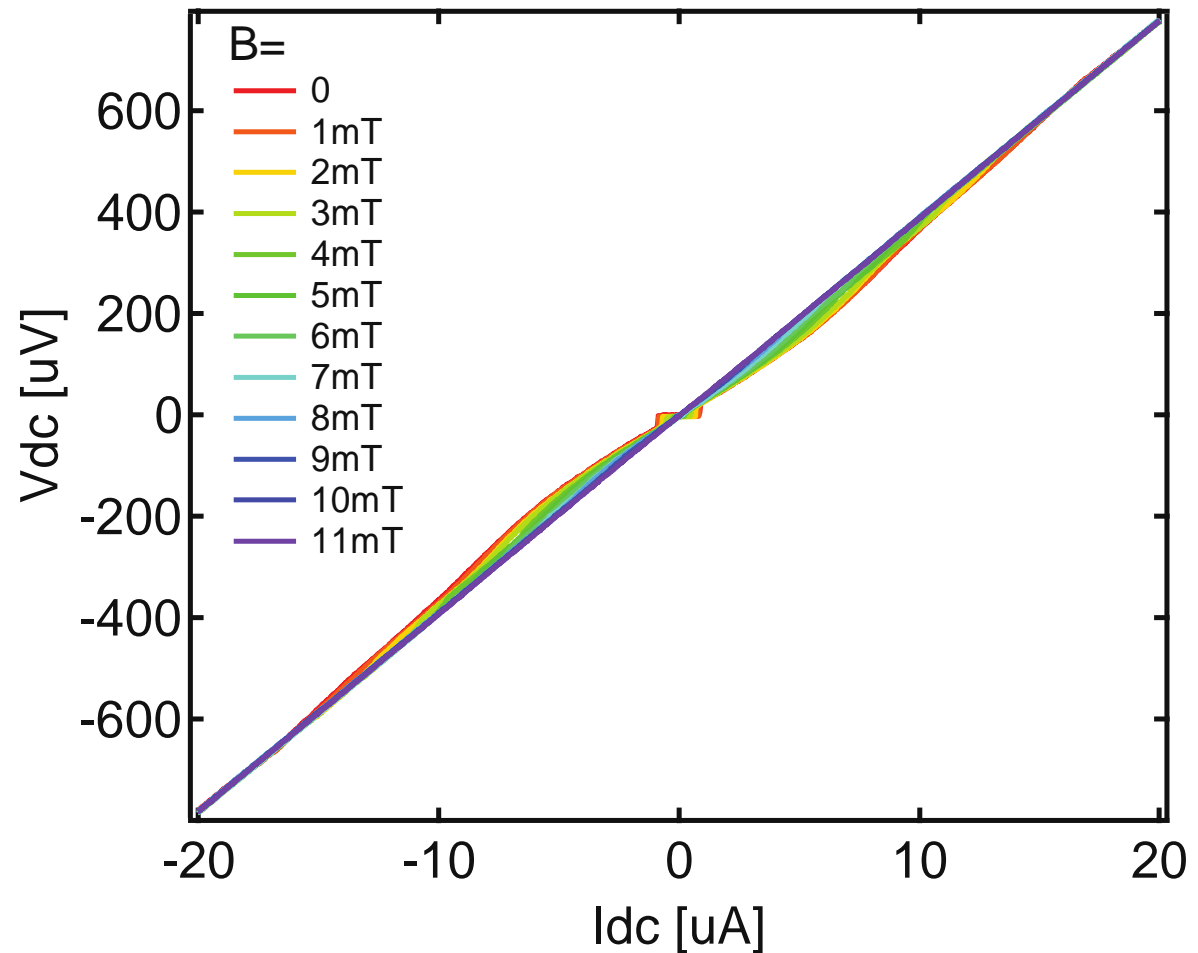
Under-Damped Junctions: Fulton-Dunkleberger

$$\langle I_C \rangle = I_{c0} \left\{ 1 - \left[\frac{E_{therm}}{2E_J} \ln \left(\frac{\omega_p \Delta t}{2\pi} \right)^{2/3} \right] \right\}$$

- Can calculate the amount of thermal fluctuations needed to reduce I_C by 90%, and you get a thermal radiation of 3.8K

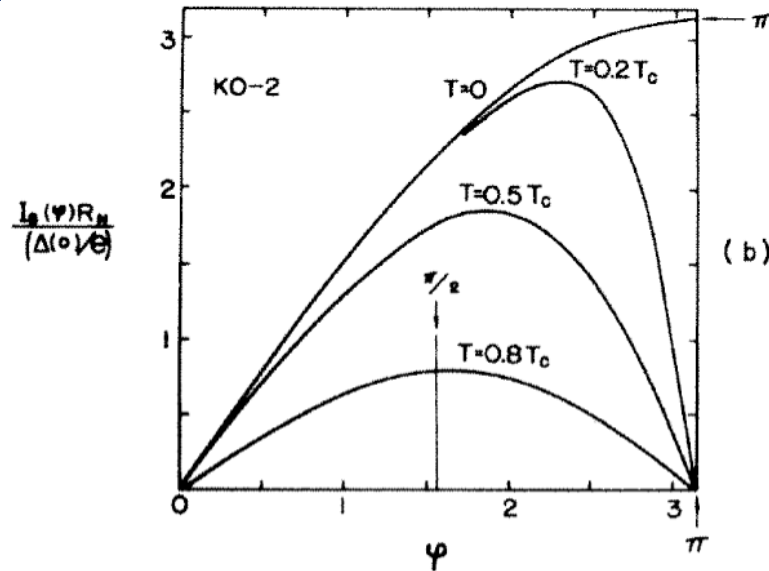
DC (higher current) vs field

- I-V curves for different magnetic fields lie on top of each other above 2Δ , $\sim 300\mu\text{V}$.



KO-2 Theory

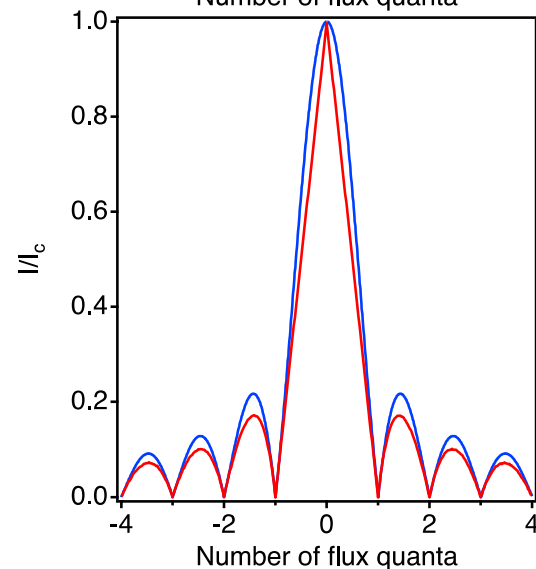
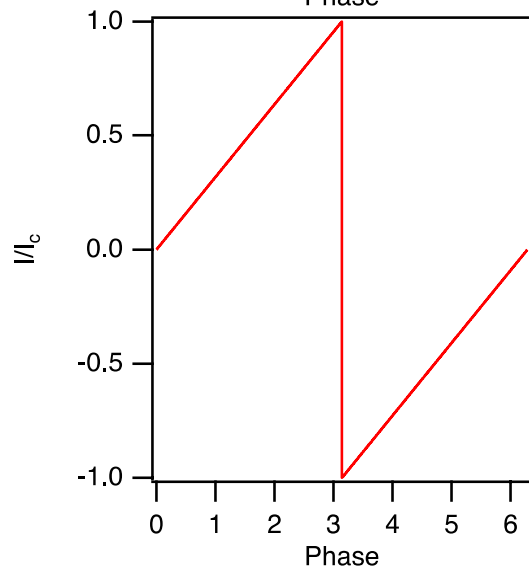
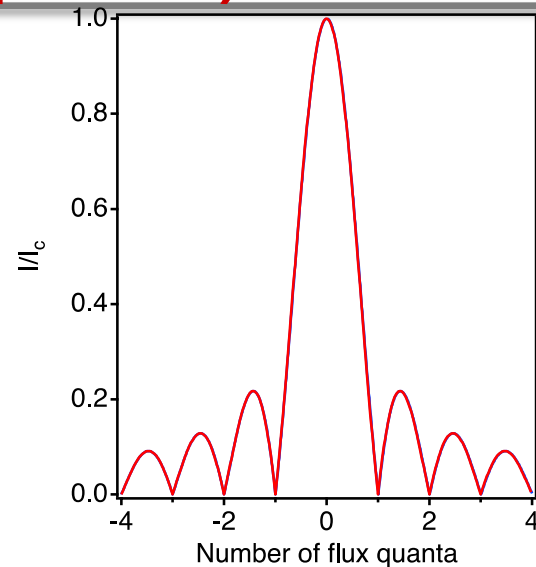
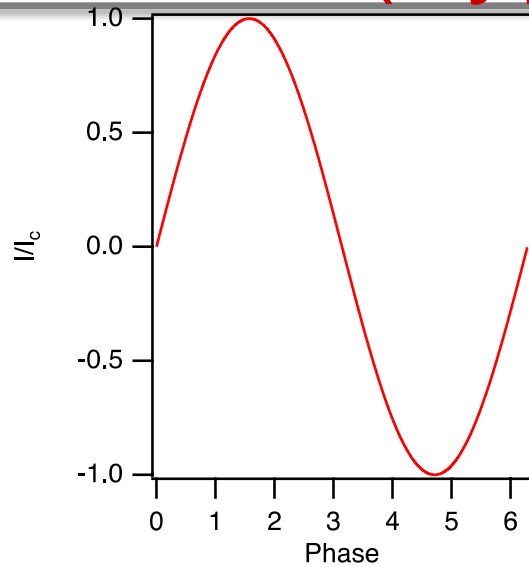
- Solutions to Eilenberger equations equations for ballistic structures (Likharev RMP 51, 101 (1979). $T=0$, peak in phase at π .



$$I_C R_N = \frac{\pi \Delta}{e} \sin\left(\frac{\varphi}{2}\right) \tanh \frac{\Delta \cos\left(\frac{\varphi}{2}\right)}{2k_B T}$$

FIG. 10. The KO-2 theory for clean small weak links ($L_{\text{eff}} \ll l, \xi_0$). (a) Two types of electron trajectories in the weak link region: (1) “incoming” part of through trajectory; (2) “outgoing” part of this trajectory; (3) and (4) nonthrough trajectories. (b) Current-phase relationship for different temperatures. Temperature dependence of critical current is shown in Fig. 6.

Current-Phase and I_c vs B (Typical)



Current-Phase and I_c vs B (Peaked)

